Plant Physiology Preview. Published on September 24, 2019, as DOI:10.1104/pp.19.00979

Short title: AKR Metabolizes Glyphosate and Confers Resistance

Author for contact: Qin Yu (qin.yu@uwa.edu.au)

Article title: Aldo-keto reductase metabolizes glyphosate and confers glyphosate resistance in *Echinochloa colona*

Author names and affiliations: Lang Pan [a, b, c, d], Qin Yu [d, *], Heping Han [d], Lingfeng Mao[e], Alex Nyporko[f], LongJiang Fan[e, *], Lianyang Bai [a, b, c, *], Stephen Powles [d]

[a]College of Plant Protection, Hunan Agricultural University, Changsha, 410128, China

[b]Hunan Weed Science Key Laboratory, Hunan Academy of Agriculture Science, Changsha, 410125, China,

[c]State Key Laboratory of Hybrid Rice, Hunan Academy of Agricultural Sciences, Changsha, 410125, China,

[d]Australian Herbicide Resistance Initiative (AHRI), School of Agriculture and Environment, University of Western Australia, Australia, WA 6009

[e]Institute of Crop Science and Zhejiang University-Xuan Gu Agricultural Joint Innovation Center, Zhejiang University, Hangzhou, 310058, China

[f]Taras Shevchenko National University of Kyiv, Kiev, Ukraine

[*]co-correspondence authors. Email: Q Yu (qin.yu@uwa.edu.au), LJ Fan (fanlj@zju.edu.cn), LY Bai (bailianyang2005@aliyun.com)

One-sentence summary: The plant metabolic enzyme aldo-keto reductase has evolved to metabolize glyphosate in a glyphosate-resistant weed species

List of author contributions: L.P., Q. Y., L. F. and L. B. designed the research; L.P., H. H., L. M. and A. N. performed the research; L.P. and Q. Y. analyzed the data; and L.P., Q. Y., A.N. and S. P. wrote the paper. Q.Y. agrees to serve as the author responsible for contact and ensures communication.

Abstract

Glyphosate, the most commonly used herbicide in the world, controls a wide range of plant species, mainly because plants have little capacity to metabolize (detoxify) glyphosate. Massive glyphosate use has led to world-wide evolution of glyphosate-resistant weed species, including the economically damaging grass weed *Echinochloa colona*. An Australian population of *E. colona* has evolved resistance to glyphosate with unknown mechanisms that do not involve the glyphosate target enzyme 5-enolpyruvylshikimate-3-phosphate synthase. Glyphosate-resistant (GR) and susceptible (S) lines were isolated from this population and used for resistance gene discovery. RNA sequencing (RNA-seq) analysis and phenotype/genotype validation experiments revealed that one aldo-keto reductase (AKR) contig had higher expression and higher resultant AKR activity in GR than S plants. Two full-length *AKR* (*EcAKR4-1* and *EcAKR4-2*) cDNA transcripts were cloned with identical sequences between the GR and S plants but were upregulated in the GR plants. Rice (*Oryza sativa*) calli and seedlings overexpressing *EcAKR4-1* and displaying increased AKR activity were resistant to glyphosate. EcAKR4-1 expressed in *E. coli* can metabolize glyphosate to produce aminomethylphosphonic acid (AMPA) and glyoxylate. Consistent with these results, GR *E. colona* plants exhibited enhanced capacity for detoxifying glyphosate into AMPA and glyoxylate. Structural modelling predicted that glyphosate binds to EcAKR4-1 for oxidation, and metabolomics analysis of *EcAKR4-1* transgenic rice seedlings revealed possible redox pathways involved in glyphosate metabolism. Our study provides direct experimental evidence of the evolution of a plant AKR that metabolizes glyphosate and thereby confers glyphosate resistance.

Key words: *Echinochloa colona*, glyphosate resistance, aldo-keto reductase (AKR), glyphosate metabolism, aminomethylphosphonic acid (AMPA)

Introduction

Glyphosate is the world's most commonly used herbicide, with estimated annual use of 300 million pounds in the USA in recent years, owing to its high efficacy, broad spectrum, and systemic mode of action (Duke et al., 2018). Despite minimal resistance evolution in weeds during the first two decades of glyphosate use, the high adoption of glyphosate tolerant transgenic crops from 1996 onwards imposed very high glyphosate selection pressure, resulting in widespread evolution of glyphosate resistance in the Americas. Since first reported (Powles et al., 1998; Pratley et al., 1999), evolution of glyphosate resistant weeds has dramatically increased, mainly in the Americas and to a lesser extent in many other parts of the world (Duke and Powles, 2008; Duke et al., 2018). Currently, 304 populations of 42 weedy species have evolved resistance to glyphosate across six continents (Heap, 2019).

Given the widespread occurrence and importance of glyphosate resistant (GR) weed evolution, the biochemical and molecular basis of mechanisms endowing glyphosate resistance is under intensive study. Both target-site and non-target-site glyphosate resistance mechanisms exist (Sammons and Gaines, 2014). Specific mutations in the target enzyme of glyphosate, 5-enolpyruvylshikimate-3-phosphate synthase (EPSPS), can endow glyphosate resistance (Baerson et al., 2002; Sammons and Gaines, 2014; Yu et al., 2015; Gaines et al., 2019). Mutations in EPSPS have been documented at amino acid position Pro106 (Sammons and Gaines, 2014), Thr102 (Li et al., 2018), Thr102+Pro106 (the "TIPS" double mutation) (Yu et al., 2015), and Thr102+Ala103+Pro106 (The "TAP-IVS" triple mutation) (Perotti et al., 2019). Additionally, many-fold increases in EPSPS gene amplification endows resistance by EPSPS overproduction (Gaines et al., 2010), and this mechanism has been reported in eight weedy species (Patterson et al., 2018). Non-target-site glyphosate resistance due to restricted glyphosate translocation (Lorraine-Colwill et al., 2002) occurs in many glyphosate resistant weed species, and likely involves increased glyphosate sequestration to vacuoles (Ge et al., 2010). However, non-target-site glyphosate resistance mechanisms have been only elucidated at the biochemical level and the molecular basis remains unknown.

Most plant species cannot significantly metabolize glyphosate, which is a major factor contributing to its lethality in plants. However, glyphosate is readily metabolized by a variety of soil microbes via a glyphosate oxidoreductase (GOX), which cleaves the glyphosate C-N bond forming amino methyl phosphonic acid (AMPA) and glyoxylate, and, to a lesser extent, via a C-P lyase, forming sarcosine and inorganic phosphate (Barrett and Mcbride, 2005; Pizzul et al., 2009). Some plant species, notably legumes, can metabolize glyphosate, especially to AMPA, but without correlation to the level of tolerance to glyphosate (Reddy et al., 2008; Duke, 2011; Nandula et al., 2019). Studies on a wide range of glyphosate-resistant (GR) weed species report no glyphosate metabolism (Sammons and Gaines, 2014). Only two reports show evidence of glyphosate metabolites (e.g. AMPA, sarocosine) in GR weeds, without further elaboration (de Carvalho et al., 2012; González-Torralva et al., 2012). Glyphosate metabolism to AMPA and glyoxylate in plants is likely due to plant GOX-like activities or horizontal gene transfer from microbes (Duke, 2011). However, neither GOX-like glyphosate-metabolizing enzymes nor their encoding genes have been identified in plant species, making their discovery a research priority (Duke, 2011).

Aldo-keto reductase (AKR) superfamilies are widely distributed in prokaryotes and eukaryotes (Barski et al., 2008; Simpson et al., 2009), and typically catalyze NAD(P)(H)-dependent reduction of aldehydes and ketones under normal or stress conditions. Due to their broad substrate specificity, AKRs can also metabolize a large number of xenobiotics (Barski et al., 2008; Simpson et al., 2009; Penning, 2015). However, plant AKRs have not been well studied, with the most characterized being the AKR4C family involved in aldehyde detoxification and stress defense, osmolyte production, secondary metabolism and membrane transport (Simpson et al., 2009; Penning, 2015). For example, AKR4C8 and AKR4C9 from *Arabidopsis thaliana* can reduce a range of toxic compounds containing reactive aldehyde groups (Simpson et al., 2009). In contrast, AKR4C7 from maize (*Zea mays*) catalyzes the oxidation of sorbitol to glucose (Sousa et al., 2009). In addition, AKR17A1 from the cyanobacterium *Anabaena* sp. PCC7120 catalyzes the metabolism of the herbicide butachlor into dicarboxylic acid and phenol (Agrawal et al., 2015). Importantly, it has been recently reported that AKR genes from *Pseudomonas* (*PSAKR1*) and rice (*Oryza*

sativa) (*OsAKR1*), when over-expressed in bacteria and tobacco (*Nicotiana tabacum*), showed improved glyphosate tolerance (Vemanna et al., 2017). However, these genes were experimentally derived, and how these AKRs detoxify glyphosate remains elusive.

Here, we used a GR *Echinochloa colona* (awnless barnyard grass) population (Gaines et al., 2012) in which the unknown glyphosate resistance mechanism is not based on the target site EPSPS and not due to reduced glyphosate uptake or translocation at the tissue level (Goh et al., 2018). Our preliminary work did not reveal glyphosate metabolism (Goh et al., 2018), but we observed that glyphosate resistance was influenced by temperature, indicating the involvement of metabolic and/or transporter proteins. In light of the work by Vemanna et al. (2017), we hypothesised that glyphosate metabolism mediated by a plant AKR may be involved in glyphosate resistance in this *E. colona* population. Using RNA-seq, we identified a novel AKR gene (designated as *EcAKR4-1*) in our GR *E. colona* population. Over-expression of *EcAKR4-1* in transgenic rice endows glyphosate resistance, and *E. coli* expressed EcAKR4-1 converts glyphosate to AMPA and glyoxylate. Glyphosate metabolism in GR vs. susceptible (S) *E. colona* plants was then re-examined using UPLC-MS/MS, which confirmed an enhanced capacity of the GR plants to detoxify glyphosate to AMPA and glyoxylate. We explored the structural interactions of EcAKR4-1 and glyphosate, and, based on these results together with a metabolomic analysis of *EcAKR4-1* transgenic rice seedlings, we propose a possible EcAKR4-1-mediated redox pathway involved in glyphosate metabolism.

Results

Consistent up-regulation of an AKR contig in GR *E. colona* plants

The GR and S individuals of a single GR (R_{single}) and a single S (S_{single}) line from within the GR *E. colona* population were selected for RNA-seq (Fig. 1). Consistent with our previous study (Goh et al., 2018), EPSPS expression was not significantly different between GR and S samples (Supplemental Table S1), excluding target-site based resistance in this population. Twelve AKR contigs were identified in RNA-seq analysis (Table S1), and expression of one AKR contig (EC_v4.g051927) was

significantly higher in GR vs. S samples and hence selected for quantitative PCR (qPCR) validation. This AKR contig showed consistently higher expression (up to 5-fold) (Table 1) in multiple GR compared to S *E. colona* lines and populations, including (1) 3 GR vs. 3 S samples used for RNA-seq, (2) an additional 6 GR vs. 6 S spare samples for RNA-seq, (3) 10 GR vs. 10 S samples each from bulked GR (R_{bulk}) and S (S_{bulk}) populations, (4) 10 GR vs. 10 S samples each from the R_{single} and S_{single} lines, and (5) 10 GR vs. 10 S samples that were isolated from within each of the R_{bulk} and R_{single} lines (Table 1). Ten samples each from the two additional S populations (QBG1 and Grossy) were also analyzed against the 10 samples from the S_{single} line, and no increased expression of the AKR contig (EC_v4.g051927) was detected (Table 1) in the supplementary S lines. These results establish that higher expression of the AKR contig (EC_v4.g051927) correlates with glyphosate resistance in *E. colona*.

Importantly, the level of glyphosate resistance in the R_{single} line was influenced by temperature. When GR *E. colona* was grown at 35/30°C, all R_{single} plants survived 540 g glyphosate ha^{-1}, but when grown at 25/20°C, only 70% survived this glyphosate rate. Similarly, temperature had an impact on plant biomass. When treated with 540 g glyphosate ha^{-1} at 35/30°C, R_{single} plants produced 95% of the biomass of untreated controls. However, at 25/20°C, R_{single} plants produced only 30% of the biomass of untreated controls. Therefore, expression of the AKR contig (EC_v4.g051927) was further tested for its response to temperature, and significantly higher expression (2.9-fold) was recorded under 35/30°C than 25/20°C growth temperatures (Table 1).

Full sequence cloning and analysis of the AKR genes

Full coding sequences of two AKR genes (*AKR1* and *AKR2*, respectively) were cloned from GR and S *E. colona*. The two transcripts had the same cDNA length (933 bp) and showed 95% identity. Due to *E. colona* being a polyploid (Supplementary Fig. S1), these may be two homeologous AKR gene alleles or copies. Therefore, two specific primers, AKR1F/AKR1R and AKR2F/AKR2R (Supplementary Table S2) for *AKR1* and *AKR2*, respectively, were designed to quantify the expression of these two transcripts in *E. colona.* As expected, a higher level of expression of both transcripts (5.1-fold for *AKR1* and 4.8-fold for *AKR2*) was detected in the GR vs. S samples used for RNA-seq.

Sequence alignment of the *AKR1* and *AKR2* genes between GR and S *E. colona* plants showed no single nucleotide polymorphisms (SNPs). In addition, *AKR1* and *AKR2* sequences from the two supplementary glyphosate susceptible *E. colona* populations (QBG1 and Crossy) were also compared with the S line. No SNPs in *AKR1*, and three SNPs in *AKR2* were found, the latter causing no amino acid changes.

Analysis using the NCBI conserved domain tool (http://www.ncbi.nlm.nih.gov/Structure/cdd/wrpsb.cgi) identified AKR domains, confirming AKR1 and AKR2 belong to the AKR family. The *E. colona* AKR1 and AKR2 amino acid sequences were 93% similar to rice OsAKR4C10 (XP_015630643.1) and sorghum (*Sorghum bicolor*) AKR4C10 (XP_002456633.1), 85% similar to maize AKR4C7 (5JH2_A) and OsAKR1 (ABF97586.1), and only 25% similar to *Pseudomonas* AKR1 (*PsAKR1*, *igrA*) (Acc. No. M37389). The nearest neighbour analysis of characterised AKR protein sequences indicates that *E. colona* AKR1 and AKR2 have close evolutionary relationships with foxtail millet (*Setaria italica*) AKR4C10, and assembled by forming a sister clade with *Oryza brachyantha* AKR4C9, and rice AKR1 and AKR2 (Supplementary Fig. S2). Based on the phylogenetic analysis, the *E. colona AKR1* and *AKR2* genes cloned in this study were designated as *EcAKR4-1* and *EcAKR4-2* (accession nos: MK592097 and MK592098), respectively (Supplementary Fig. S2).

Untranslated region (UTR) variations of the *EcAKR4* gene

To assess possible underlying mechanisms for elevated AKR expression in GR *E. colona* plants, a 264-bp 5′-UTR located between the transcription start site and translation initiation site, and a 3′-UTR region of 216 bp from the translation stop site were obtained from five plants of each GR, S and two supplementary S populations (QBG1 and Crossy). Sequence alignment showed only two SNPs in the 3′-UTR, and 10 in the 5′-UTR region between the GR and three S populations (Supplementary Fig. S3), indicating that the 5′-UTR may be involved in the regulation of expression and translation of *EcAKR4-1.*

Determination of AKR activity in *E. colona*

To determine if higher *EcAKR4* expression results in higher AKR activities, typical

AKR activities (i.e. as reductases) were measured in GR vs S plants (Table 2) against a commonly used substrate, methylglyoxal. Higher (up to 3.2-fold) AKR activities were recorded in the GR than in the S plants, consistent with the higher *EcAKR4* gene expression (up to 4.9-fold) in GR plants.

Rice calli overexpressing *EcAKR4-1* are less sensitive to glyphosate

As *EcAKR4-1* showed a slightly higher identity to Os*AKR1* (85%) (Vemanna et al., 2017), and had a higher expression relative to *EcAKR4-2*, *EcAKR4-1* was prioritised for functional confirmation using rice genetic transformation. Growth of rice calli overexpressing the *EcAKR4-1* and *GFP* (the latter used as a negative control) genes were compared on glyphosate containing medium. Growth of *GFP*-overexpressing rice calli was visibly inhibited at 0.5 mM glyphosate, and there was no growth at 1 mM glyphosate or higher (Fig. 2a). However, *EcAKR4-1*-overexpressing rice calli were less sensitive to glyphosate, with growth occurring at up to 4 mM glyphosate (Fig. 2a). It is evident that rice calli with *EcAKR4-1* overexpression exhibit resistance to glyphosate, in comparison to the rice calli over-expressing the *GFP* control.

In contrast, rice calli overexpressing *EcAKR4-1* and *GFP* were equally susceptible to the non-selective herbicide glufosinate (Supplementary Fig. S4), suggesting that EcAKR4-1 overproduction is not a general defense mechanism but a specific resistance mechanism to glyphosate selection.

Rice seedlings overexpressing *EcAKR4-1* are glyphosate resistant

Twelve re-generated T_0 rice seedlings/transformants overexpressing the *EcAKR4-1* or *GFP* gene were used for further testing. RT-qPCR using primer pairs A1/A2 and B1/B2, and sequencing analysis confirmed transcription of the *EcAKR4-1* or *GFP* gene in these 24 transgenic rice seedlings. Results showed that the *EcAKR4-1* gene was expressed 8.5-fold higher in *EcAKR4-1*-overexpressing rice seedlings relative to the *GFP*-overexpressing rice seedling controls. Correspondingly, *EcAKR4-1*-overexpressing rice seedlings had a higher (5.6-fold) level of AKR activity (against methylglyoxal) than that of *GFP*-overexpressing rice seedlings (Table 2). As expected, the *GFP*-overexpressing rice plants were killed by foliar-applied glyphosate at rates of 540 g ha^{-1} or higher. However, the *EcAKR4-1*-overexpressing rice seedlings

survived 540 and 1080 glyphosate g ha^{-1} but died at 2160 g glyphosate ha^{-1} (Fig. 2b). In addition, a total of 55 T1 seedlings from five *EcAKR4-1* transgenic lines were screened at a glyphosate rate of 540 g ha^{-1} (Fig. 2c), and the resistance and susceptibility segregated at 42:13, fitting to a single gene control mode of 3:1 (X^2=0.05, p=0.82). These results clearly establish that overexpression of *EcAKR4-1* in transgenic rice enhances AKR activity, conferring glyphosate resistance.

***In vitro* glyphosate metabolism by *E. coli* expressed EcAKR4-1 enzyme**

The ability of EcAKR4-1 to degrade glyphosate was assessed using enzyme purified from transgenic *E. coli*. SDS-PAGE analysis showed that the EcAKR4-1 enzyme was isolated as a single band around 35 kDa, close to the deduced molecular weight of the EcAKR4-1 protein (Supplementary Fig. S5). The purified EcAKR4-1 enzyme, displaying the typical AKR ability to reduce the substrate methylglyoxal (88.5±9.6 µmol mg^{-1} protein min^{-1}), was incubated with glyphosate and the resulting products were analyzed by HPLC-Q-TOF-MS. Standards of glyphosate and its possible metabolites (AMPA, glyoxylate, sarcosine and formaldehyde) were resolved in the detection system (Fig. 3, sarcosine and formaldehyde not shown).

Analysis of the enzyme reaction mix showed that in addition to glyphosate, two peaks with retention times of 1.19 min and 1.38 min, corresponding to those of the AMPA and glyoxylate standards, respectively, were detected only in the presence of the EcAKR4-1 enzyme (Fig. 3). The mass spectra of the two metabolites were also the same as those of the AMPA (m/z=112.0152) and glyoxylate (m/z=133.0146) standards. In contrast, sarcosine and formaldehyde were not detected in the incubation mixture. Clearly, purified EcAKR4-1 could metabolize glyphosate *in vitro*. In seeking optimal conditions for *in vitro* glyphosate metabolism by purified EcAKR4-1, we found that AMPA production was low in the presence of NADPH but 23-fold higher with $NADP^+$ (Table 3). Addition of $NADP^+$/NADPH only marginally increased AMPA production compared to NADPH. In contrast, replacement of $NADP^+$/NADPH by boiled water extract of plant tissue dramatically enhanced AMPA production by 633-fold compared to $NADP^+$ alone (Table 3), indicating the need for unknown plant tissue factors.

Therefore, plant tissue extract was used in the reaction mixture. Under these

conditions, glyphosate conversion to AMPA and glyoxylate occurred such that by 5h after treatment (HAT), glyphosate (1.48 mM) was completely converted to AMPA and glyoxylate (Fig. 3, Fig. 4 and Table 4). In contrast, no glyphosate metabolites were ever detected in controls at any time point (Fig. 3, Table 4). In addition and in support of the plant growth and EcAKR4-1 expression results, glyphosate conversion to AMPA by *E. coli* expressed EcAKR4-1 was enhanced at higher temperatures. For example, AMPA concentrations were 44%, 88%, 37%, and 34% higher at 35°C than at 25°C, at 1, 3, 5, and 7 HAT, respectively (Fig. 4 and Table 4). Interestingly, changes in glyoxylate concentration did not follow the same trend (Fig. 4 and Table 4), indicating the possibility of further degradation to other compounds (e.g. glycine), which was not examined in this work. The conversion of glyphosate to AMPA by EcAKR4-1 enzyme is time (Fig. 4b) and glyphosate concentration dependent (Fig. 5). The *K*m (glyphosate) was estimated to be 81 ± 4 µM, and the *Vmax* 4.79 ±0.039 µmol mg^{-1} protein min^{-1}, under our reaction conditions.

In vivo glyphosate metabolism by _E. colona_ plants

Glyphosate metabolism in above ground tissue of GR and S *E. colona* plants was analyzed using high resolution UPLC-MS/MS at 48 and 72 h after foliar application of glyphosate at a rate of 67.5 g ha^{-1} (one eighth of the field recommended rate), to avoid damage to the S plants. Results showed that the glyphosate level decreased and AMPA/glyoxylate increased with time in both GR and S plants (Table 5). However, GR plants metabolized glyphosate to AMPA more rapidly than did the S plants. For example, at 72 h after glyphosate treatment, a glyphosate to AMPA ratio of 1:4.8 and 1:0.44 as detected in GR and S plants, respectively, giving an 11-fold difference.

3D modelling reveals structural interactions of EcAKR4-1 and glyphosate

Structural modelling predicts that glyphosate interacts with EcAKR4-1 in the area involving amino acid residues Trp21, Tyr49, Lys78 and Trp112, as well as pyridine nucleotide ($NADPH/NADP^+$) molecules bound to EcAKR4-1. The predicted glyphosate binding on the EcAKR4-1 surface potentially takes at least two types of conformation (Fig. 6a and Fig. 6b). In the Type 1 conformation, glyphosate directly contacts residues Trp21, Tyr49, Lys78 and Trp112, forming attractive charge

interactions with the side chain amino groups of Lys78, including one conventional H-bond with the Tyr49 hydroxyl group, two conventional H-bonds with the side chain of Trp112, and up to six Pi interactions (two Pi-cations and four Pi-anions) with the indole of Trp21 (Fig. 6a and Fig. 6b). Glyphosate also forms Pi anion interactions with the NADP pyridine group (Fig. 6c). This type of glyphosate binding by EcAKR4-1 is not time-stable, and there was a tendency for glyphosate to be released from the EcAKR4-1 active site over the first 30 ns of molecular dynamics (MD) as glyphosate-EcAKR4-1 interaction energy rose over the studied MD interval from -138.12 kJ mol^{-1} to 0. This, however, is not critical because such a time interval is more than sufficient for glyphosate to be involved in the reaction.

In the Type 2 conformation, glyphosate immediately contacts residues Trp21, Tyr49, His111 and Trp112 as well as NADP (Fig. 6d). In this case, glyphosate forms two conventional H-bonds with Trp112, one with His111 and one with Tyr49, and two Pi cation and two Pi anion interactions with Trp21. In this conformation the van der Waals contact between glyphosate carbon-bound hydrogen and NADP pyridine was also observed (Fig. 6d and Fig. 6e). This contact is very important as the hydrogen (in fact, a hydride ion, H^-) is potentially able to be transferred to pyridine and, thus, reduce $NADP^+$ to NADPH. In contrast to the Type 1 conformation, the EcAKR4-1:$NADP^+$:glyphosate complex of the Type 2 conformation is time-stable over the 100 ns MD interval. Glyphosate-EcAKR4-1 interaction energy in this case stabilized at the level of -212.682 kJ mol^{-1} and, thus, the Type 2 glyphosate-EcAKR4-1 interaction is more likely than the Type 1. The complexes of NADPH and $NADP^+$ with EcAKR4-1 were also highly stable, did not dissociate during the 100 ns period of MD, and had appropriate values of interaction energy (-832.12 and -875.46 kJ mol^{-1}, respectively).

Metabolomic analysis of transgenic rice indicates a possible pathway for EcAKR4-1-mediated glyphosate metabolism

Metabolomic analysis was performed with and without glyphosate treatment of the transgenic rice plants. Possible glyphosate metabolites (AMPA, glyoxylate, sarcosine and formaldehyde) and the metabolic pathways involving these compounds were the main focus of the analysis. Although glyphosate and glyoxylate

were not detected in the metabolome, the level of AMPA was significantly higher in glyphosate-treated *EcAKR4-1* over-expressing (EcAKR4-1-T) versus glyphosate-treated *GFP*-overexpressing (GFP-T) rice plants, and in EcAKR4-1-T versus untreated (EcAKR4-1-C) rice plants (Table 6), confirming an increased capacity of *EcAKR4-1*-overexpressing rice plants to metabolize glyphosate. In addition, the level of glycine was greater in EcAKR4-1-T versus GFP-T and versus EcAKR4-1-C samples (Table 6), but lower in GFP-T versus untreated *GFP*-overexpressing (GFP-C) and EcAKR4-1-C versus GFP-C samples. Interestingly, it was also found that the level of cinnamaldehyde and cinnamyl alcohol showed an opposite trend among glyphosate treated/untreated *EcAKR4-1*- and GFP-overexpressing rice samples. When an increase in the level of cinnamyl alcohol was observed in EcAKR4-1-T samples relative to GFP-T and EcAKR4-1-C samples, a corresponding decrease in cinnamaldehyde was detected (Table 6). This indicates that an enhanced level of cinnamaldehyde/cinnamyl alcohol is likely associated with *EcAKR4-1* overexpression in rice plants.

Metabolites with significant changes among comparisons were mapped to the reference canonical pathway in the Kyoto Encyclopedia of Genes and Genomes (KEGG). The most attractive KEGG reaction is R00372 (glycine:2-oxoglutarate aminotransferase), converting glyoxylate to glycine. Glyoxylate, glycine, 2-oxoglutarate and L-glutamate are four compounds involved in the reaction. In fact, when a marginal increase in the abundance of 2-oxoglutarate was observed in EcAKR4-1-T relative to EcAKR4-1-C and GFP-T samples, a decrease in L-glutamate was detected (Table 6), suggesting that the glyphosate metabolite glyoxylate is further metabolized to glycine, likely coupled with 2-oxoglutarate reduction to L-glutamate in transgenic rice overexpressing *EcAKR4-1*. In fact, an increase in the glycine pool was only evident in glyphosate-treated *EcAKR4-1*-overexpressing samples (Table 6). All these results helped facilitate a hypothesis for an EcAKR4-1-catalysed glyphosate metabolism pathway in plants (Fig. 7).

Discussion

Revealing the molecular basis of non-target-site herbicide resistance mechanisms (NTSR) is challenging as it may involve superfamilies of metabolic enzymes and transporters (Délye et al., 2013) and requires multiple analytical approaches. Here, combining transcriptomic, transgenic and metabolomic approaches, we reveal that glyphosate metabolism (to AMPA) via an up-regulated plant AKR (EcAKR4-1) is involved in conferring glyphosate resistance in a GR *E. colona* population. However, how the AKR expression and activity in the GR *E. colona* plants (Table 2) are up regulated remains to be elucidated. We speculate that it may be related to SNPs in the 5'-UTR region (Supplementary Fig. S3), and post-translational modifications of the AKR, as two of the key residues (Tyr49 and Lys78) interacting with glyphosate (Fig 6c) are located relatively close to the N-terminus and are well known to display post-translational modifications (e.g. phosphorylation). Future work including promotor analysis and copy number variation of the AKR gene may provide more information on AKR gene expression regulation. And purification of the native AKR enzyme could reveal post-translational modifications.

To establish if EcAKR4-1 endows glyphosate resistance due to its ability to metabolize glyphosate, studies were conducted on *E. coli* expressed EcAKR4-1. HPLC-Q-TOF-MS analysis revealed that EcAKR4-1 catalyzes glyphosate conversion to the much less toxic compound AMPA (and glyoxylate) in a time, concentration and temperature dependent manner (Table 4 and Fig. 3, Fig. 4, Fig. 6). The estimated *K*m (glyphosate) value of EcAKR4-1 (81 ± 4 μM) was close to that determined with Arabidopsis AKR4C8 (64 ± 15 μM) and AKR4C9 (27.8 ± 13.6 μM) for oxidation of the substrate 5-dihydro-testosterone (Simpson et al., 2009). The bacterial GOX (YP_001369824.1) and GO (CP011882.1) were reported to convert glyphosate into AMPA and glyoxylate (Barry and Kishore, 1995; Mattia et al., 2009). However, the EcAKR4-1 that we identified in the current study showed only 23.5% homology to GOX and 27.7% to GO, indicating that EcAKR4-1 might be a novel plant GOX-like enzyme. Indeed, consistent with the metabolomics analysis of glyphosate metabolism in AKR transgenic rice (Table 6), analysis of glyphosate metabolism in GR vs S *E. colona* plants demonstrated that GR plants have greater capacity to convert glyphosate to AMPA and glyoxylate than the S plants (Table 5). AMPA is much less phytotoxic than glyphosate (Nandula et al., 2007; Duke, 2011), but still has some

herbicidal activity, and therefore plants possessing only the ability to metabolize glyphosate to AMPA have not completely detoxified glyphosate. Although the other glyphosate metabolite, glyoxylate (also an endogenous metabolite in plant photorespiration), is known to be inhibitory to ribulose-1-5-biphosphate carboxylase/oxygenase (Lu et al., 2014), it may be detoxified to glycolate by glyoxylate reductase, and to glycine by glycine: 2-oxoglutarate aminotransferase as observed in EcAKR4-1 transgenic rice (see Results on metabolomics). Genetic inheritance of glyphosate resistance in this particular GR *E. colona* population has not been investigated yet. However, NTSR-based herbicide resistance can be a polygenic (quantitative) trait (Duhoux et al., 2015). Based on our preliminary studies, an additional resistance mechanism (e.g. ABC transporters) may sequester glyphosate/AMPA away from the target enzyme EPSPS in the cytoplasm.

To explore the structural basis of AKR-catalyzed conversion of glyphosate, we employed 3D modelling of EcAKR4-1. This protein belongs to the NADP-dependent AKR family, which usually uses NADPH as an electron source for substrate reduction (Penning, 2015). However, one NADPH molecule is able to donate only two electrons (one hydride anion, H^-). To reduce the carboxyl group of glyphosate to an alcohol, at least four electrons (two hydride anions) are necessary. EcAKR4-1 is able to bind only one NADPH molecule, and exchange of $NADP^+$/NADPH molecules during the reaction cycle is practically impossible because the nucleotide is more deeply buried in the protein space than glyphosate. In order to bind the second NADPH molecule, the EcAKR4-1 would have to release the incompletely processed substrate. Hence, glyphosate reduction by EcAKR4-1 using NADPH as a cofactor may be structurally unlikely to occur. Rather, glyphosate oxidation by EcAKR4-1 may be possible, similar to the known mechanism of GOX or GO by soil micro-organisms (Pollegioni et al., 2011). In fact, the ability of plant AKRs to oxidize several substrates has been demonstrated (Kavanagh et al., 2002; Simpson et al., 2009; Sousa et al., 2009). Among other possibilities, the oxidized form of NADP ($NADP^+$) is an acceptable substitute. This is supported by the fact that addition of $NADP^+$ rather than NADPH in the *in vitro* reaction greatly enhanced glyphosate conversion to AMPA (Table 3). As EcAKR4-1 also displayed a typical AKR activity reducing the substrate methylglyoxal, it may have a dual redox function (e.g. reducing the substrate of some

445 aldehydes/ketones and oxidizing the substrate like glyphosate), although with much
446 higher reducing than oxidizing activity (88.5±9.6 versus 4.79±0.039 μmol mg^{-1}
447 protein min^{-1}, respectively). The presence of two substrates (i.e. glyphosate and an
448 aldehyde/ketone) or other unknown components or cofactors would accelerate the
449 change of NADP state from $NADP^+$ to NADPH and vice versa, and, as a result,
450 increase the productivity of the reactions. This was realized by a dramatic increase in
451 AMPA production upon addition to the reaction mixture of plant tissue extracts that
452 may contain these compounds (Fig. 3, Fig. 4 and Table 3). The cofactors/substrates in
453 plant tissue extract that putatively enhance AKR activity need further investigation.

454 To understand possible pathways for EcAKR4-1 mediated glyphosate
455 metabolism, a metabolomic analysis of *EcAKR4-1* transgenic rice was performed. The
456 most relevant changes in metabolite abundance were a significant increase in
457 2-oxoglutarate and cinnamyl alcohol and a decrease in L-glutamate and
458 cinnamaldehyde in glyphosate-treated EcAKR4-1 (EcAKR4-1-T) plants (Table 6). This
459 coincided with an increased level of the glyphosate metabolites AMPA and glycine in
460 these plants, suggesting that the reduction of cinnamaldehyde to cinnamyl alcohol
461 could be coupled with glyphosate oxidation to AMPA, and reduction of
462 2-oxoglutarate to L-glutamate linked with glyoxylate conversion to glycine. Thus, we
463 propose a hypothetical metabolic pathway that EcAKR4-1 works as a dual
464 oxidase/reductase in a cycle catalyzing glyphosate oxidation and cinnamaldehyde
465 reduction using the same NADP molecule as both an acceptor and a donor of
466 electrons (Fig. 7). Although our data (Table 3 and 6, Fig. 6) are consistent with this
467 hypothetical model, further experimental validation is needed.

468 Glyphosate is rarely metabolized by plants. However, all possible resistance
469 mechanisms, including rare mechanisms, are selected by persistent glyphosate
470 selection pressure on huge weed populations across vast areas. GOX-like plant
471 enzymes have been long suspected to evolve in response to glyphosate selection,
472 but have received little attention (Duke, 2011). In the present study, we demonstrate
473 that increased expression of an AKR gene (*EcAKR4-1*) has been selected by intensive
474 glyphosate use and endows this *E. colona* population with an enhanced capacity to
475 metabolize and thus resist glyphosate. Our findings will open a new avenue for
476 studies on metabolic herbicide resistance, additional to P450 and GST mediated

herbicide metabolism (Powles and Yu, 2010; Yu and Powles, 2014). It is worthwhile to examine the potential evolution of AKR mediated metabolic resistance to glyphosate (and other herbicides) in other herbicide resistant weedy plant species.

Materials and Methods

Plant materials

To minimize genetic variability, the initially bulked GR (R_{bulk}) and susceptible (S_{bulk}) lines were obtained from within a single GR *Echinochloa colona* population by vegetative plant cloning plus glyphosate treatment (Goh et al., 2016). We established that glyphosate resistance in this R_{bulk} line is non-target-site based (Goh et al., 2018). Single R (R_{single}) and S (S_{single}) lines were then generated respectively from the initial R_{bulk} and S_{bulk} lines for the present study (Fig. 1) (Goh et al., 2018). This process further minimized genetic variability between the GR and S *E. colona* lines for RNA-seq analysis. In addition, as the R_{bulk} and R_{single} lines are still segregating for glyphosate resistance at 2X the recommended field rate of 1080 g glyphosate ha^{-1} (resistance:susceptibility 22:3), this allows for further isolation of GR and S individuals (R_{bulk}-R/S, R_{single}-R/S) from within each of these two R lines for contig expression validation (Fig. 1). Furthermore, plants from two additional glyphosate-susceptible *E. colona* populations (QBG1 and Crossy) from north-east Australia were also included for contig expression analysis.

The GR and S individuals were determined by glyphosate treatment. Briefly, GR and S seedlings were grown in pots in a controlled environment room with day/night temperature of 35/30°C and light flux of 350 µmol m^{-2} s^{-1} at 75% humidity. At the 1–2-tiller stage, the above-ground (1 cm) shoot and leaf material of individual plants were removed, snap-frozen in liquid nitrogen and stored at -80 °C. Three days later the GR seedlings were treated with 1080 g glyphosate ha^{-1} and the S seedlings with 270 g glyphosate ha^{-1}. Glyphosate was applied using a laboratory spray cabinet with a two-nozzle boom delivering 118 L ha^{-1} water at a pressure of 210 kPa and a speed of 1 m s^{-1}. Plant survival was determined two weeks after treatment, and the most GR and the S individuals were identified and the corresponding pre-harvested frozen shoot material was used for RNA-seq.

508

509 **RNA-seq data analysis and AKR gene expression validation**

510 Detailed descriptions of the RNA-seq data analysis, PCR validation of the AKR
511 gene expression in RNA-seq samples and samples from multiple GR and S
512 populations/lines, and under different temperatures, are provided in Supplementary
513 Information-2.

514

515 **Full sequence cloning and analysis of the AKR genes**

516 Based on *Echinochloa crus-galli* genome sequences, one primer pair, EcAKR-F
517 (5'-CTTCCTAAAGTTCACCGTCCCA-3') / EcAKR-R (5'-CCACCACCACTGCTTCCCT-3'), was
518 designed from the UTR for cloning the full-length cDNA sequences of *E. colona* AKR
519 genes. PCR was conducted in a 25 µL volume, consisting of 1 µL cDNA, 0.5 mM of
520 each primer and 12.5 µL of PrimeSTAR MAX (Takara). PCR was run in a Mastercycler
521 (ABI) with the following profile: 98 °C 10 s, 40 cycles of 98 °C 10 s, 56 °C 15 s, and
522 72 °C 90 s, followed by a final extension step of 7 min at 72 °C. The amplified cDNA
523 fragments were purified from agarose gels using the 'Wizard SV gel and PCR clean-up
524 system (Promega). The amplified cDNA fragment was cloned into the pGEM-T vector
525 (Promegam, Madison, WI) and transformed into *E. coli* competent cells (strain
526 JM109). The chromatogram files of all sequences were visually checked, and
527 sequences were aligned using the DNAMAN software.

528 5'-Rapid amplification of cDNA ends (5'-RACE) and 3'-RACE were conducted to
529 clone the UTR region of the *EcAKR4-1* gene from plants of the R and three S *E. colona*
530 populations using the SMART RACE kit (Takara, Japan) with gene specific primers of
531 EcAKR-51/EcAKR-52 for 5'-RACE and EcAKR-31/EcAKR-32 for 3'-RACE
532 (Supplementary Table S2).

533

534 **Measurement of AKR activity in *E. colona***

535 AKR activities in plants of R_{bulk}, R_{single}, S_{bulk}, S_{single}, and two other S *E. colona*
536 populations (QBG1 and Crossy), were determined using a commercial kit (Zhenao
537 Corporation, China) with methylglyoxal as a substrate according to the
538 manufacturer's instructions. AKR was extracted by grinding 0.4 g leaf material in
539 liquid nitrogen with 400 µL of isolation buffer, followed by centrifugation at 13,000 g

for 10 min. The reaction mixture contained 0.1 M sodium phosphate buffer (pH 7), 0.1 mM of NADPH/NADH, 2 mM methylglyoxal and 400 µL leaf extract (3.6 mg protein). AKR activity was quantified by measuring the decrease in NADPH concentration at 340 nm over 3 min using a Shimadzu (Kyoto, Japan) UV-160 spectrophotometer at 25 °C.

Rice calli transformation and growth response to glyphosate

To express *EcAKR4-1* in rice calli, expression cassettes were constructed as described in Fig. S6. The vectors were introduced into *Agrobacterium tumefaciens* by electroporation and the transformed *A. tumefaciens* strains were used to transform WT (wild type) Nipponbare rice. All constructed vectors were checked carefully by restriction analysis and DNA sequencing prior to rice transformation.

Rice transformation was carried out using the procedures as described in (Seiichi et al., 2010), with modifications. The introduction of the transgene into rice calli was confirmed by PCR using the primer pair HygF1 (5'-GACCTGCCTGAAACCGAACTG-3')/HygR1 (5'-CCCAAGCTGCATCATCGAAA-3'), which amplifies the HPT gene in the vector. Hygromycin-resistant rice calli were selected, and sub-cultured in Nutrient Broth (NB) plates (with hygromycin), and proliferating calli transferred onto fresh NB plates containing glyphosate at 0, 0.5, 1, 2, 4 and 8 mM (stock solution prepared in water). Glyphosate concentrations at ≥ 0.5 mM inhibited growth of the GFP-transgenic rice calli (used as a negative control). For each glyphosate concentration, 10 transformed calli were used and two independent transformation experiments were conducted. After two weeks in the dark, the growth response to glyphosate was compared between calli transformed with the GFP or the *EcAKR4-1* gene. In addition, the response of transgenic calli to the non-selective herbicide glufosinate was also tested at concentrations of 0, 10, 40, 80 and 120 µM.

Glyphosate sensitivity of transgenic rice seedlings

Transgenic rice (*Oryza sativa*) calli (GFP and *EcAKR4-1* overexpressing lines) were regenerated and T_0 plantlets ranging from 3 to 5 cm in length were transferred to rooting medium supplemented with hygromycin. After 7 days of acclimatisation,

572 the T_0 seedlings were transferred to a mixture of fertilised soil and perlite (2:1, v/v)
573 for subsequent molecular analysis and glyphosate resistance testing.

574 Seedlings were screened first by PCR using the specific primer pair HygF1/HygR1
575 for the vector HPT gene. For further detection of the target transgene, two primer
576 pairs were designed: A1 (5'-AAAGAAATTGGGTGACTTG-3') and A2
577 (5'-CTTGTAAACGCTCTGTGG-3') amplifying a 427-bp fragment of transformed
578 *EcAKR4-1*, and B1 (5'-TTGTCCCAGTTCTCATTG-3') and B2
579 (5'-GTATCTTGCGAAACATCTAA-3') amplifying a 373-bp fragment of transformed GFP.
580 *EcAKR4-1* gene expression and total AKR activity were quantified as described above
581 and in Supplementary Information 2. The seedlings were grown in a controlled
582 growth cabinet with an average day/night temperature of 30/25°C and a 14-h
583 photoperiod under a light intensity of 180 µmol m^{-2} s^{-1}. T_0 seedlings of 12 lines were
584 then foliar treated with glyphosate at 0, 540, 1080 and 2160 g ha^{-1} (corresponding to
585 0, 1X, 2X and 4X the recommended field rate), respectively, and T1 seedlings of 5
586 lines were treated at 540 g ha^{-1}. Glyphosate was applied using a 3WP-2000
587 hand-held system (Nanjing, China), equipped with a 390 mL min^{-1} flow nozzle at a
588 pressure of 3.0 kg cm^{-2}. Plant survival and mortality was determined three weeks
589 after treatment.

590

591 ***EcAKR4-1* gene expression in *E. coli* and *in vitro* glyphosate metabolism assay**

592 To determine if the EcAKR4-1 gene product can metabolize glyphosate, the
593 *EcAKR4-1* gene was expressed with a hexahistidine tag in *E. coli* using the expression
594 system pET32a. The His-tagged EcAKR4-1 enzyme was purified using the MagneHis
595 Protein Purification System (Promega Co., Madison, USA). Cells were lysed directly in
596 the culture medium using the provided FastBreak Cell Lysis Reagent. His-tagged
597 EcAKR4-1 enzyme was purified under native conditions. The protein was dissolved
598 with the lysis buffer (FastBreak Cell Lysis Reagent, pH 7.4) and quantified using the
599 Bradford method (Bradford, 1976).

600 This purified enzyme was used for glyphosate metabolism studies. The reaction
601 mixture (3 mL, pH 6.8) was 9 µg EcAKR4-1 enzyme, 1.48 mM glyphosate (prepared in
602 water), and 0.3 mL aqueous plant tissue extract (20 g *E. colona* plant material in 500
603 ml water, extracted in boiling water for 10 min and filtered) to supplement any

604 unknown factors (e.g. cofactors) for the AKR enzyme reaction. The reaction mixture
605 was incubated for 1, 3, 5, and 7 h at 25 °C and 35 °C, respectively. HPLC-Q-TOF-MS
606 analysis (see below) was performed to detect reaction products at each time point.
607 Mixtures of glyphosate and plant tissue extract without AKR enzyme served as the
608 control. In addition, a mixture of *E. coli* expressed His-tagged BSA protein, glyphosate
609 and plant tissue extract was used as a vector control.

610 To estimate AKR *K*m and *Vmax* for glyphosate, EcAKR4-1 enzyme (20 µg), and
611 glyphosate at 1, 10, 100, 500, 1000, 1500 and 2000 µM were used. The reactions
612 were incubated at 35 °C for 30 min and AMPA production was measured using
613 HPLC-Q-TOF-MS. The *K*m value was calculated by fitting the data to the
614 Michaelis–Menten equation $v = VS/(Km + S)$. Each assay contained two technical
615 replicates and the assay was repeated three times with similar results, and data were
616 pooled for analysis.

617

618 **HPLC-Q-TOF-MS analysis of glyphosate metabolites by *E. coli* expressed EcAKR4-1**
619 **enzyme**

620 Chromatographic separations of glyphosate and its possible metabolites (AMPA,
621 glyoxylate, sarcosine and formaldehyde) were achieved with the 1290 HPLC system
622 (Agilent Technologies, Palo Alto, CA, USA) on a XAqua C_{18} column (2.1 mm × 150 mm,
623 particle size 5 µm, Acchrom, China). The mobile phase consisted of 0.1% (v/v) formic
624 acid (FA) aqueous solution (solvent A) and acetonitrile (ACN) (solvent B) with a flow
625 rate of 0.3 mL min^{-1} and an injection volume of 5 µL. The gradient was set as 0-5 min
626 with an isocratic elution of 10% (v/v) solvent B.

627 Mass spectral analysis was carried out using an Agilent Technologies mass
628 spectrometer (6530 QqTOF MS). The eluent from the HPLC was directed into the
629 mass spectrometer through an electrospray ionization interface and data were
630 acquired in full scan mode (m/z: 20-1000 Da). Glyphosate and AMPA data acquisition
631 were performed in positive ionization, and glyoxylate in negative ionization mode.
632 Parameters of the ion source were: gas temperature 345 °C, gas flow 10 L min^{-1},
633 nebuliser 40 psi, sheath gas temp 350 °C, sheath gas flow 11 L min^{-1}, vcap voltage
634 4000 V, nozzle voltage 500 V, and fragment voltage 135 V. Accurate mass
635 measurements of each peak from the total ion chromatogram were obtained using

an automated calibration to provide the mass correction. Purine ($C_5H_4N_4$, *m/z*: 121.0508, Agilent, USA) and HP-0921 ($C_{18}H_{18}O_6N_3P_3F_{24}$, *m/z*: 922.0097, Agilent, USA) were used for mass calibration. Monoisotopic masses of the protonated molecular ions $[M+H]^+$ were calculated using the data explorer software of the Q-TOF instrument. HPLC-Q-TOF-MS data were processed using the Agilent Masshunter Qualitative Analysis software (B.05.00). The calibration equations were established from known concentrations of analytical grade of glyphosate and its metabolites, which were determined from their peak areas in the electropherogram. The experiment had three replicates and was repeated with similar results, and all data were pooled for analysis.

UPLC-MS/MS analysis of glyphosate metabolites by GR and S *E. colona* plants

GR and S *E. colona* plants were grown under the same conditions as for transgenic rice plants. At the 3- to 4-leaf stage they were treated with glyphosate at 67.5 g ha^{-1}, using the 3WP-2000 hand-held system described above. Above ground tissue samples were collected 48 and 72 h after treatment, and unabsorbed glyphosate was removed by rinsing the samples in 100 mL DL water and blotting dry. After extraction with water under ultrasonication, the sample was defatted with dichloromethane and purified on a C_{18} solid phase extraction cartridge, and then glyphosate, APMA and glyoxylate were derivatised using 9-fluorenylmethoxycarbonyl (FMOC-Cl) in borate buffer for 2 h. The derivatives of glyphosate, APMA and glyoxylate were separated by gradient elution on a Waters UPLC BEH C_{18} column with the mobile phase of 2 mmol L^{-1} ammonium acetate and acetonitrile, and detected by positive eletrospray ionisation-mass spectrometry (ESI^+-MS/MS) in multiple reaction monitoring (MRM) mode. The derivatives of glyphosate, APMA and glyoxylate were used as standards for sample quantification. The experiment was conducted with eight biological replicates per harvest and each replicate sample consisted of five plants. Other possible glyphosate metabolites (e.g. sarcosine and formaldehyde) were not analyzed.

Structural modelling of EcAKR4-1

The spatial structure of *E. colona* AKR was reconstructed based on the EcAKR4-1

sequence by a homology modelling approach (Venselaar et al., 2010) using the SWISS-MODEL web-service (Waterhouse et al., 2018). The 1.00 Å resolution crystal structure of *Homo sapiens* aldose reductase in complex with NADP (Protein Data Bank ID 2AGT) and 1.45 Å resolution crystal structure of AKR4C7 from maize (*Zea mays*) (PDB ID 5JH1) were used as templates for EcAKR4-1 reconstruction based on the highest scores among all possible structural templates. Computational details are according to procedures described in our previous work (Chu et al., 2018) and in Supplementary information-2.

Metabolomics analysis of transgenic rice seedlings

The experimental design for metabolomic analysis included eight biological replicates of transgenic rice seedlings overexpressing *EcAKR4-1* or GFP, with and without glyphosate treatment at 270 g ha^{-1}. Leaf samples of untreated controls were collected at time point 0, and glyphosate-treated samples were collected 24 h after treatment. The leaf samples were homogenized in 80% methanol and 0.1% (v/v) FA, vortexed and sonicated for 10 min and stored at -20 °C for 1 h prior to overtaxing at room temperature and centrifugation at 18407 g for 20 min at 4 °C. The supernatant (1 mL) was filtered through a 0.22-µm organic phase filter into a glass vial before use. An Accucore HILIC column was used for liquid chromatography, at 40 °C and a flow rate of 3 mL min^{-1}. In positive phase liquid chromatography, the mobile phase A was 95% (v/v) ACN and 0.1% FA, and B was 50% (v/v) ACN and 0.1% FA. In negative phase liquid chromatography, A was 95% ACN (pH 9.0), and the mobile phase B was 50% ACN (pH 9.0). The gradient was: 98% A:2% B for one minute, a linear gradient to 50% A:50% B over 17.5 min, and 2 min isocratic before going back to the initial LC conditions in 20 min. Ten µL of each sample were injected and a flow rate of 0.2 mL min^{-1} was used throughout the LC runs. Metabolites were quantified by normalization to the internal standards. Other technical details, and data analysis are provided in Supplementary information-2.

Accession numbers

The *EcAKR4-1* and *EcAKR4-2* sequences have been deposited in the GenBank database (accession nos: MK592097 and MK592098).

Supplemental Data

Supplemental material-1

Supplementary Fig. S1 Somatic chromosome counting of *Echinochloa colona* (4n=36) using root tip samples.

Supplementary Fig. S2 Phylogenetic analysis of EcAKR4-1 and EcAKR4-2 and their relationships with other plant AKRs.

Supplementary Fig. S3 Sequence comparison of the amplified fragments of (a) the 3' UTR and (b) the 5'UTR from *E. colona* plants of the GR, S and two additional S populations (QBG1 and Crossy).

Supplementary Fig. S4 Growth of rice calli transformed with the *GFP* or *EcAKR4-1* genes in medium containing glufosinate.

Supplementary Fig. S5 SDS-PAGE analysis of recombinant EcAKR4-1 enzyme purified from *E. coli*.

Supplementary Fig. S6 Vector construct for over-expression of *EcAKR4-1* in rice callus.

Supplementary Table S1. Identification of differentially expressed aldo-keto reductase (AKR) and EPSPS contigs in glyphosate resistant (GR) vs. susceptible (S) populations of *Echinochloa colona* using RNA-seq.

Supplementary Table S2. Primers used for RT-qPCR relative quantification of gene expression and UTR cloning.

Supplemental material-2

Materials and methods related to RNA-seq data analysis and AKR gene expression

validation, structural modelling of EcAKR4-1 and metabolomic analysis.

Acknowledgments

This work was financially supported by the National Natural Science Foundation of China (31901905 and U19A200212), the Australian Grains Research and Development Corporation (GRDC), China Agriculture Research System (CARS-16-E19), the Zhejiang Natural Science Foundation (LZ17C130001), the Jiangsu Collaborative Innovation Center for Modern Crop Production, the 111 Project (B17039), and the award (TG-DMR 110088) from the Extreme Science and Engineering Discovery Environment (XSEDE). We are grateful to Dr SS Goh for his initial characterization of this GR *E. colona* population, and Dr Danica Goggin for proofreading of the manuscript.

Tables

Table 1. Validation of the *Echinochloa colona* candidate aldo/keto reductase (AKR) contig (EC_v4.g051927) using a series of pre-phenotyped samples. R: glyphosate resistant, S: glyphosate susceptible.

Sample sources	Relative expression Ratio (R/S) [a]	p-value	Significance[b]
RNA-seq results	2.2	0.0001	**
Validation using RNA-seq samples	4.9	0.006	**
Validation using spare RNA-seq samples	4.8	0.0043	**
Validation using population/line samples			
R_{bulk}/S_{bulk}	4.6	0.0069	**
R_{single}/S_{single}	4.8	0.0365	*
R_{bulk}-R/R_{bulk}-S	2.0	0.0277	*
R_{single}-R/R_{single}-S	2.5	0.0265	*
QBG1 (S) /S_{single}	0.9	0.2076	
Crossy (S)/S_{single}	1.0	0.8469	
R_{single} (35/30°C)/ R_{single} (25/20°C)	2.9	0.0004	**

[a] Raw FPKM (fragments per thousand bases per million reads) reads for the RNA-seq results, and RT-qPCR validation for all others.

[b] *P*-value <0.05, 0.01 indicated by *, **, respectively (t-test).

Table 2. AKR activities measured using methylglyoxal as a substrate in glyphosate resistant (GR) vs susceptible (S) lines/populations of *Echinochloa colona*, and T_0 transgenic rice seedlings. Data are means ± SE (n=3)

Material	EcAKR activity (µmol mg^{-1} min^{-1})
R plants from R_{single}	5.8 (0.18)
R plants from R_{bulked}	5.5 (0.23)
S plants from S_{single}	2.2 (0.11)
S plants from S_{bulked}	2.3 (0.17)
S plants-QBG1 population	1.8 (0.14)
S plants-Crossy population	2.5 (0.09)
EcAKR4-1-overexpressing T_0 rice seedlings	7.8 (0.22)
GFP-overexpressing T_0 rice seedlings	1.4 (0.17)

Table 3 *In vitro* production of the glyphosate metabolite AMPA by *E. coli* expressed EcAKR4-1 enzyme in the reaction mixture (3 mL), as affected by respective addition of the following ingredients, 3h after incubation with glyphosate at 25 °C. Data are means ± SE (n=3)

Ingredient in the reaction mix	pH	AMPA (µg mL^{-1})
NADPH (0.1 mM)	7.4	0.149 (0.006)
$NADP^+$ (0.1 mM)	5.8	3.436 (0.095)
$NADP^+$/NADPH (0.1 mM)	6.5	3.955 (0.058)
$NADP^+$/NADPH (0.1 mM)	7.5	4.219 (0.168)
Plant tissue (0.3 mL boiled water extract)	6.8	94.33 (1.209)
Plant tissue (0.3 mL) + $NADP^+$/NADPH (0.1 mM of each)	6.7	95.09 (2.432)

Table 4. HPLC-Q-TOF-MS analyses of glyphosate metabolites produced by the action of *E. coli* expressed EcAKR4-1 at different temperatures. Data are means ± (SE) (n=6)

	Hours after treatment	25 °C (µg ml^{-1})			35 °C (µg ml^{-1})		
		Glyphosate	AMPA	Glyoxylate	Glyphosate	AMPA	Glyoxylate
Control[a]	1	241 (2.4)	0	0	245 (12.9)	0	0
	3	249 (15.4)	0	0	246 (9.4)	0	0
	5	238 (14.7)	0	0	242 (10.3)	0	0
	7	245 (4.0)	0	0	244 (26.4)	0	0
Vector control[b]	1	235 (12.2)	0	0	243 (2.1)	0	0
	3	246 (10.5)	0	0	245 (17.6)	0	0
	5	249 (12.9)	0	0	237 (8.5)	0	0
	7	248 (16.3)	0	0	235 (11.1)	0	0
EcAKR4-1[c]	1	164 (13.1)	58.4 (5.8)	13.6 (2.4)	165 (8.0)	84.3 (1.2)	21.8 (1.3)

3	89.6 (1.4)	99.5 (2.9)	37.6 (1.4)	46.6 (3.1)	187 (5.9)	35.8 (1.8)
5	0	178 (7.0)	56.9 (0.8)	0	244 (1.8)	60.0 (1.4)
7	0	177 (14.4)	65.1 (1.0)	0	237 (10.3)	64.8 (3.0)

[a] Glyphosate was mixed with plant tissue extract .

[b] Bacterial expressed vector control BSA protein was mixed with glyphosate and plant tissue extract.

[c] Bacterial expressed EcAKR4-1 protein was mixed with glyphosate and plant tissue extract.

Table 5. UPLC-MS/MS analyses of glyphosate metabolites in glyphosate resistant (GR) vs. susceptible (S) populations of *Echinochloa colona*. The 3- to 4-leaf stage plants were treated with glyphosate at 67.5 g ha^{-1}. Data are means ± (SE) (n=8)

Time point	Population	Glyphosate (μg g^{-1})	AMPA (μg g^{-1})	Glyoxylate (μg g^{-1})
Untreated	S	0	0	2.0 (0.2)
	GR	0	0	1.2 (0.1)
48h	S	44.4 (3.9)	8.8 (1.3)	8.8 (1.0)
	GR	34.6 (4.2)	20.6 (2.7)	15.4 (1.4)
72h	S	37.9 (3.6)	16.6 (0.9)	13.5 (1.3)
	GR	9.0 (1.7)	43.3 (1.8)	32.7 (3.1)

Table 6. Changes in abundance of relevant metabolites identified by partial least square discriminant analysis (PLS-DA) and significance analysis. C: control, T: glyphosate treated.

Metabolites	EcAKR4-1-C/GFP-C		EcAKR4-1-T/ EcAKR4-1-C		GFP-T/GFP-C		EcAKR4-1-T/GFP-T	
	Fold change[a]	*P*	Fold change [a]	*P*	Fold change [a,b]	*P*	Fold change [a,b]	*P*
Aminomethylphosphonic acid (AMPA)	1	-	2.7*	0.020	1	-	3.7**	0.003
Cinnamaldehyde	1	-	- 3.1*	0.037	1	-	- 3.3*	0.013
Cinnamyl alcohol	1	-	3.1**	0.005	- 3.0**	0.008	3.3**	0.001
Glycine	-3.6**	0.001	3.1**	0.005	-3.0**	0.005	2.7*	0.023
2-oxoglutarate	1	-	3.7*	0.029	6.7*	0.045	2.8**	0.004
L-glutamate	1	-	-2.9**	0.010	1	-	-3.8*	0.013

[a] *P*-value <0.05, 0.01 indicated by *, **, respectively (Tukey's test).

[b] Fold change of 1 indicates no change, negative values indicate down-regulation.

Figure Legends

Fig. 1 Population resources used for RNA-seq and validation in the present study.

Fig. 2 Overexpression of *EcAKR4-1* confers glyphosate resistance in rice. Growth response to glyphosate of rice calli (a), T_0 (b) and T_1 (c) seedlings transformed with the *GFP* (control) or *EcAKR4-1* gene, three weeks after glyphosate treatment. Note only glyphosate surviving T1 seedlings from *EcAKR4-1* overexpressing lines are shown in (c).

Fig. 3 HPLC-Q-TOF-MS analyses of glyphosate metabolism catalyzed by *E. coli* expressed EcAKR4-1. (a) 1 and (b) 5 h after *in vitro* incubation. Standard: analytical grade glyphosate, aminomethylphosphonic acid (AMPA), and glyoxylate. Control: mixture of glyphosate and plant tissue extract. Vector control: mixture of *E. coli* expressed BSA protein, glyphosate and plant tissue extract. EcAKR4-1: mixture of *E. coil* expressed EcAKR4-1 enzyme, glyphosate and plant tissue extract.

Fig. 4 Time-dependent glyphosate metabolism by *E. coli* expressed EcAKR4-1. (a) glyphosate breakdown, and (b) accumulation of glyphosate metabolites aminomethylphosphonic acid (AMPA) and (c) glyoxylate in mixtures of *E. coli* expressed EcAKR4-1 and plant tissue extract. Data are means ±SE (*n*=6).

Fig. 5 Concentration-dependent accumulation of AMPA in response to increased glyphosate concentrations in the mixture of *E.coli* expressed EcAKR4-1 enzyme and plant tissue extract. Data are means ±SE (*n*=6).

Fig. 6 3D modelling reveals structural interactions of EcAKR4-1 and glyphosate. General view of EcAKR4-1 with bound $NADP^+$ (stick representation colored in green) and glyphosate (ball and stick representation) in (a) Type 1 conformation, and (b) Type 2 conformation. (c) Spatial structure of contact interface between glyphosate and EcAKR4-1 in the type 1 conformation (left, NADP molecule is not present) and 2D-diagram (right) of intermolecular interactions. The protein contact surface is colored by H-bond donor/acceptor distribution, binding site amino acids are represented by sticks, and intermolecular contacts are indicated by dotted lines. (d)

Spatial structure of the contact interface between glyphosate and EcAKR4-1 in the type 2 conformation (left, NADP molecule is not present) and 2D-diagramm of intermolecular interactions (right). The protein contact surface is colored by H-bond donor/acceptor distribution, binding site amino acids are represented by sticks, and intermolecular contacts are indicated by dotted lines. (e) Partially presented relative spatial orientation of glyphosate (right) and $NADP^+$ (left). The distance between the transferable hydrogen and target carbon in the NADP composition is shown by a red line.

Fig. 7 Proposed metabolic pathway demonstrating the dual oxidase/reductase activity of EcAKR4-1 involved in glyphosate metabolism in *E. colona*. Glyphosate is oxidized to aminomethylphosphonic acid (AMPA) by EcAKR4-1 using $NADP^+$ as a cofactor, and meanwhile cinnamaldehyde is reduced to cinnamyl alcohol, regenerating $NADP^+$. Glyoxylate produced by glyphosate oxidation is further converted to glycine by transaminase coupled with L-glutamate reduction to 2-oxoglutarate with NADPH as a cofactor. X indicates cleavage of the C-N bond in the glyphosate molecule. Please note that our structural modelling (Fig 6), *in vitro* glyphosate metabolism by *E. coli* expressed *EcAKR4-1* (Table 3), and metabolomics of *EcAKR4-1* transgenic rice (Table 6) are consistent with the proposed step for glyphosate conversion to AMPA. Further conversion of glyoxylate to glycine was only based on the metabolomic analysis of *EcAKR4-1* transgenic rice (Table 6). Nevertheless, further experimental validation is needed for the proposed pathway.

Literature Cited

Agrawal C, Sen S, Yadav S, Rai S, Rai LC (2015) A novel aldo-keto reductase (AKR17A1) of *Anabaena sp.* PCC 7120 degrades the rice field herbicide butachlor and confers tolerance to abiotic stresses in *E. coli*. Plos One **10:** e0137744

Baerson SR, Rodriguez DJ, Minhtien T, Yongmei F, Biest NA, Dill GM (2002) Glyphosate-resistant goosegrass. Identification of a mutation in the target enzyme 5-enolpyruvylshikimate-3-phosphate synthase. Plant Physiol **129:** 1265-1275

Barrett KA, Mcbride MB (2005) Oxidative degradation of glyphosate and aminomethylphosphonate by manganese oxide. Environ Sci **39:** 9223-9228

Barry GF, Kishore GM (1995) Glyphosate tolerant plants. US patent 5, 463, 175

Barski OA, Tipparaju SM, Bhatnagar A (2008) The aldo-keto reductase superfamily and its role in drug metabolism and detoxification. Drug Metab Rev **40:** 553-624

Bradford MMA (1976) A rapid and sensitive method for the quantitation on microgram quantities of protein utilizing the principle of protein-dye binding. Anal Biochem **72:** 248–254

Chu Z, Chen J, Nyporko A, Han H, Yu Q, Powles S (2018) Novel α-tubulin mutations conferring resistance to dinitroaniline herbicides in *Lolium rigidum*. Front Plant Sci **9**

de Carvalho LB, Alves PLdCA, González-Torralva F, Cruz-Hipolito HE, Rojano-Delgado AM, De Prado R, Gil-Humanes J, Barro F, Luque de Castro MD (2012) Pool of resistance mechanisms to glyphosate in *Digitaria insularis*. J Agric Food Chem **60:** 615-622

Délye C, Jasieniuk M, Le Corre V (2013) Deciphering the evolution of herbicide resistance in weeds. Trends Genet **29:** 649-658

Duhoux A, Carrère S, Gouzy Jm, Bonin L, Délye C (2015) RNA-Seq analysis of rye-grass transcriptomic response to an herbicide inhibiting acetolactate-synthase identifies transcripts linked to non-target-site-based resistance. Plant Mol Biol **87:** 473-487

Duke SO (2011) Glyphosate degradation in glyphosate-resistant and -susceptible crops and weeds. J Agric Food Chem **59:** 5835-5841

Duke SO, Powles SB (2008) Glyphosate: a once-in-a-century herbicide. Pest Manag Sci **64:** 319-325

Duke SO, Powles SB, Sammons RD (2018) Glyphosate-How it became a once in a hundred year herbicide and its future. Outlooks on Pest Manag **29:** 247-251

Gaines TA, Cripps A, Powles SB (2012) Evolved resistance to glyphosate in Junglerice (*Echinochloa colona*) from the tropical ord river region in Australia. Weed Technol **26:** 480-484

Gaines TA, Patterson EL, Neve P (2019) Molecular mechanisms of adaptive evolution revealed by global selection for glyphosate resistance. New Phytol doi:10.1111/nph.15858

Gaines TA, Zhang W, Wang D, Bukun B, Chisholm ST, Shaner DL, Nissen SJ, Patzoldt WL, Tranel PJ, Culpepper AS, Grey TL, Webster TM, Vencill WK, Sammons RD, Jiang J, Preston C, Leach JE, Westra P (2010) Gene amplification confers glyphosate resistance in *Amaranthus palmeri*. Proc Natl Acad Sci U S A **107:** 1029-1034

Ge X, d'Avignon DA, Ackerman JJH, Sammons RD (2010) Rapid vacuolar sequestration: the horseweed glyphosate resistance mechanism. Pest Manag Sci **66:** 345-348

Goh SS, Vila-Aiub MM, Busi R, Powles SB (2016) Glyphosate resistance in *Echinochloa colona*: phenotypic characterisation and quantification of selection intensity. Pest Manag Sci **72:** 67-73

Goh SS, Yu Q, Han H, Vila-Aiub MM, Busi R, Powles SB (2018) Non-target-site glyphosate resistance in *Echinochloa colona* from Western Australia. Crop Prot **112:** 257-263

González-Torralva F, Rojano-Delgado AM, Luque de Castro MD, Mülleder N, De Prado R (2012) Two non-target mechanisms are involved in glyphosate-resistant horseweed (*Conyza canadensis* L. Cronq.) biotypes. J Plant Physiol **169:** 1673-1679

Heap I (2019) International survey of herbicide resistant weeds [online]. *In*, Vol 2019, http: //www.weedscie nce.org

Kavanagh KL, Mario K, Bernd N, Wilson DK (2002) The structure of apo and holo forms of xylose reductase, a dimeric aldo-keto reductase from *Candida tenuis*. Biochem **41:** 8785

Li J, Peng Q, Han H, Nyporko A, Kulynych T, Yu Q, Powles S (2018) A novel EPSPS Thr-102-Ser substitution endows glyphosate resistance in Tridax procumbens. Journal of Agricultural & Food Chemistry

Lorrainecolwill, D. F, Powles, S. B, Hawkes, T. R, Hollinshead, P. H, Warner, S. AJ (2002) Investigations into the mechanism of glyphosate resistance in *Lolium rigidum*. Pestic Biochem Phys **74:**

62-72
Lu Y, Li Y, Yang Q, Zhang Z, Chen Y, Zhang S, Peng X-X (2014) Suppression of glycolate oxidase causes glyoxylate accumulation that inhibits photosynthesis through deactivating Rubisco in rice. Physiol Plantarum **150:** 463-476
Mattia P, Elena R, Gianluca M, Tommaso M, Carmelinda S, Beatrice V, Loredano P (2009) Glyphosate resistance by engineering the flavoenzyme glycine oxidase. J Biol Chem **284:** 36415
Nandula VK, Reddy KN, Rimando AM, Duke SO, Poston DH (2007) Glyphosate-resistant and -susceptible soybean (*Glycine max*) and canola (*Brassica napus*) dose response and metabolism relationships with glyphosate. J Agric Food Chem **55:** 3540-3545
Nandula VK, Riechers DE, Ferhatoglu Y, Barrett M, Duke SO, Dayan FE, Goldberg-Cavalleri A, Tétard-Jones C, Wortley DJ, Onkokesung N, Brazier-Hicks M, Edwards R, Gaines T, Iwakami S, Jugulam M, Ma R (2019) Herbicide metabolism: crop selectivity, bioactivation, weed resistance, and regulation. Weed Sci **67:** 149-175
Patterson EL, Pettinga DJ, Ravet K, Neve P, Gaines TA (2018) Glyphosate resistance and EPSPS gene duplication: Convergent evolution in multiple plant species. J Hered **109:** 117-125
Penning TM (2015) The aldo-keto reductases (AKRs): overview. Chem Biol Interact **234:** 236-246
Perotti VE, Larran AS, Palmieri VE, Martinatto AK, Alvarez CE, Tuesca D, Permingeat HR (2019) A novel triple amino acid substitution in the EPSPS found in a high-level glyphosate-resistant *Amaranthus* hybridus population from Argentina. Pest Manage Sci **75:** 1242-1251
Pizzul L, Castillo MDP, Stenström J (2009) Degradation of glyphosate and other pesticides by ligninolytic enzymes. Biodegradation **20:** 751-759
Pollegioni L, Schonbrunn E, Siehl D (2011) Molecular basis of glyphosate resistance-different approaches through protein engineering. Febs Journal **278:** 2753-2766
Powles SB, Lorrainecolwill DF, Dellow JJ, Preston C (1998) Evolved resistance to glyphosate in rigid ryegrass (*Lolium rigidum*) in Australia. Weed Sci **46:** 604-607
Powles SB, Yu Q (2010) Evolution in action: plants resistant to herbicides. Annu Rev Plant Biol **61:** 317-347
Pratley J, Stanton R, Urwin N, Baines P, Hudson D, Dill G, Bishop AC, Boersma M, Barnes CD (1999) Resistance to glyphosate in *Lolium rigidum*. I. Bioevaluation. Weed Sci **47**: 405-411
Reddy KN, Rimando AM, Duke SO, Nandula VK (2008) Aminomethylphosphonic acid accumulation in plant species treated with glyphosate. J Agric Food Chem **56:** 2125
Sammons RD, Gaines TA (2014) Glyphosate resistance: state of knowledge. Pest Manag Sci **70:** 1367-1377
Seiichi T, Naho H, Kazuko O, Haruko O, Akemi T, Seibi O, Hiroshi T (2010) Early infection of scutellum tissue with Agrobacterium allows high-speed transformation of rice. Plant J **47:** 969-976
Simpson PJ, Tantitadapitak CReed AM, Mather OC, Bunce CM, White SA, Ride JP (2009) Characterization of two novel aldo-keto reductases from Arabidopsis: expression patterns, broad substrate specificity, and an open active-site structure suggest a role in toxicant metabolism following stress. J Mol Biol **392:** 465-480
Sousa SMD, Rosselli LK, Kiyota E, Silva JCD, Souza GHMF, Peroni LA, Stach-Machado DR, Eberlin MN, Souza AP, Koch KE (2009) Structural and kinetic characterization of a maize aldose reductase. Plant Physiol Bioch **47:** 98-104
Vemanna RS, Vennapusa AR, Easwaran M, Chandrashekar BK, Rao H, Ghanti K, Sudhakar C, Mysore KS, Makarla U (2017) Aldo-keto reductase enzymes detoxify glyphosate and improve herbicide resistance in plants. Plant Biotechnol J **15:** 794-804
Venselaar H, Joosten RP, Vroling B, Baakman CAB, Hekkelman ML, Krieger E, Vriend G (2010) Homology modelling and spectroscopy, a never-ending love story. Eur Biophy J **39:** 551-563
Waterhouse A, Bertoni M, Bienert S, Studer G, Tauriello G, Gumienny R, Heer FT, De TB, Rempfer C, Bordoli L (2018) SWISS-MODEL: homology modelling of protein structures and complexes. Nucleic Acids Res **46:** W296-W303
Yu Q, Jalaludin A, Han H, Chen M, Sammons RD, Powles SB (2015) Evolution of a double amino acid substitution in the 5-Enolpyruvylshikimate-3-Phosphate synthase in *Eleusine indica* conferring high-level glyphosate resistance. Plant Physiol **167:** 1440-1447
Yu Q, Powles S (2014) Metabolism-based herbicide resistance and cross-resistance in crop weeds: A threat to herbicide sustainability and global crop production. Plant Physiol **166:** 1106-1118

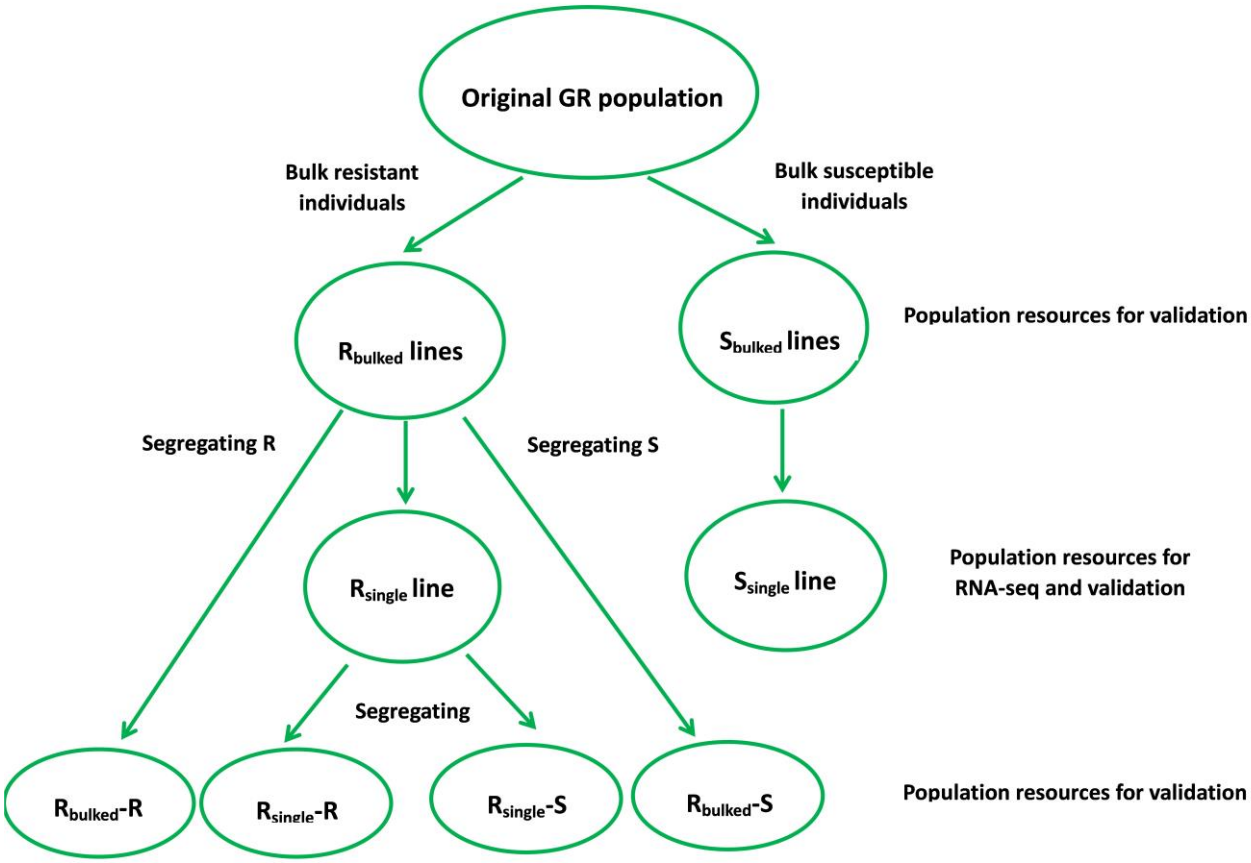

Fig. 1 Population resources used for RNA-seq and validation in the present study.

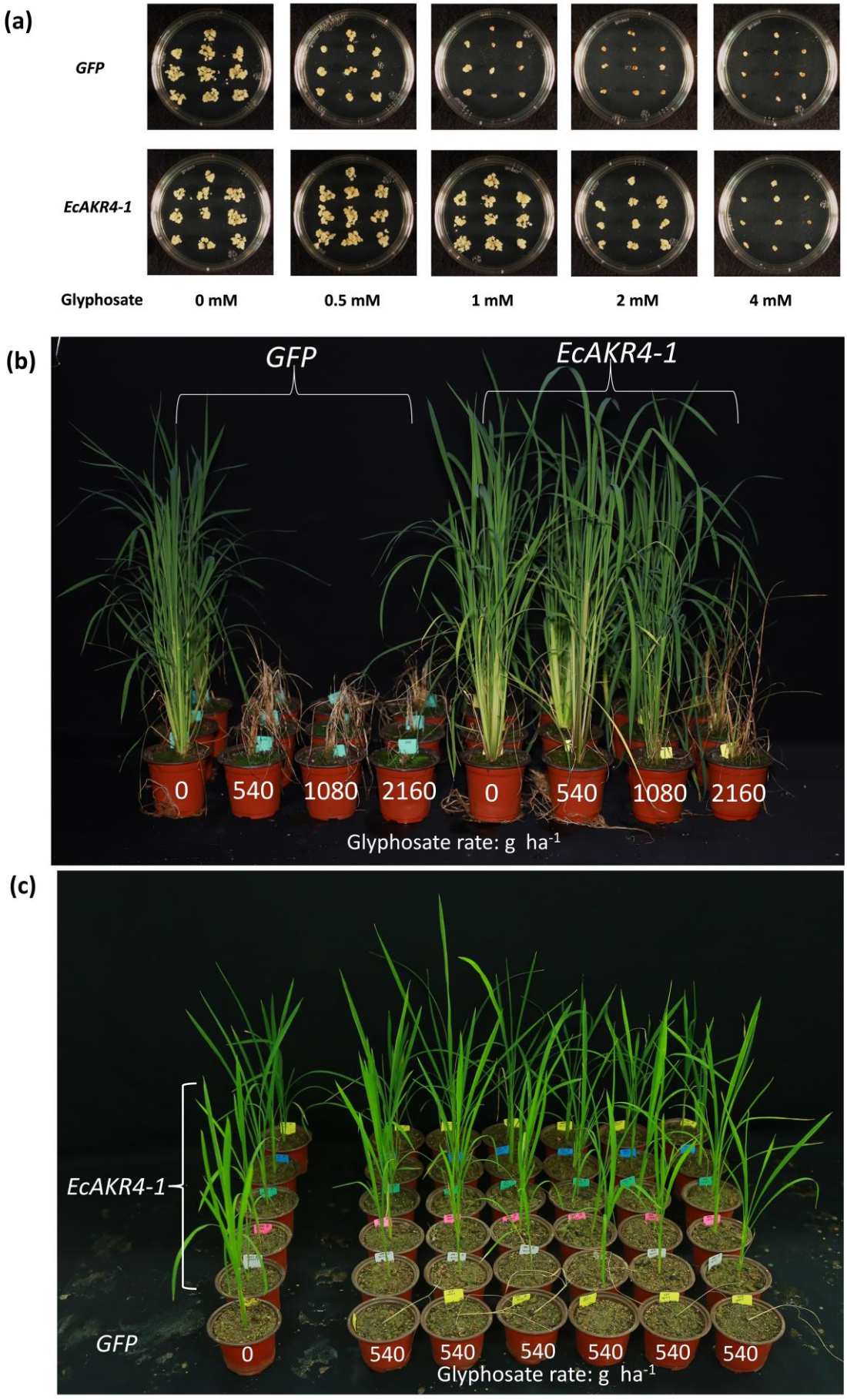

1

Fig. 2 Overexpression of the *EcAKR4-1* gene confers glyphosate resistance in rice. Growth response to glyphosate of rice calli (a), T_0 (b) and T_1 (c) seedlings transformed with the *GFP* (control) or *EcAKR4-1* gene, three weeks after glyphosate treatment. Note only glyphosate surviving T1 seedlings from *EcAKR4-1* overexpressing lines were shown in (c).

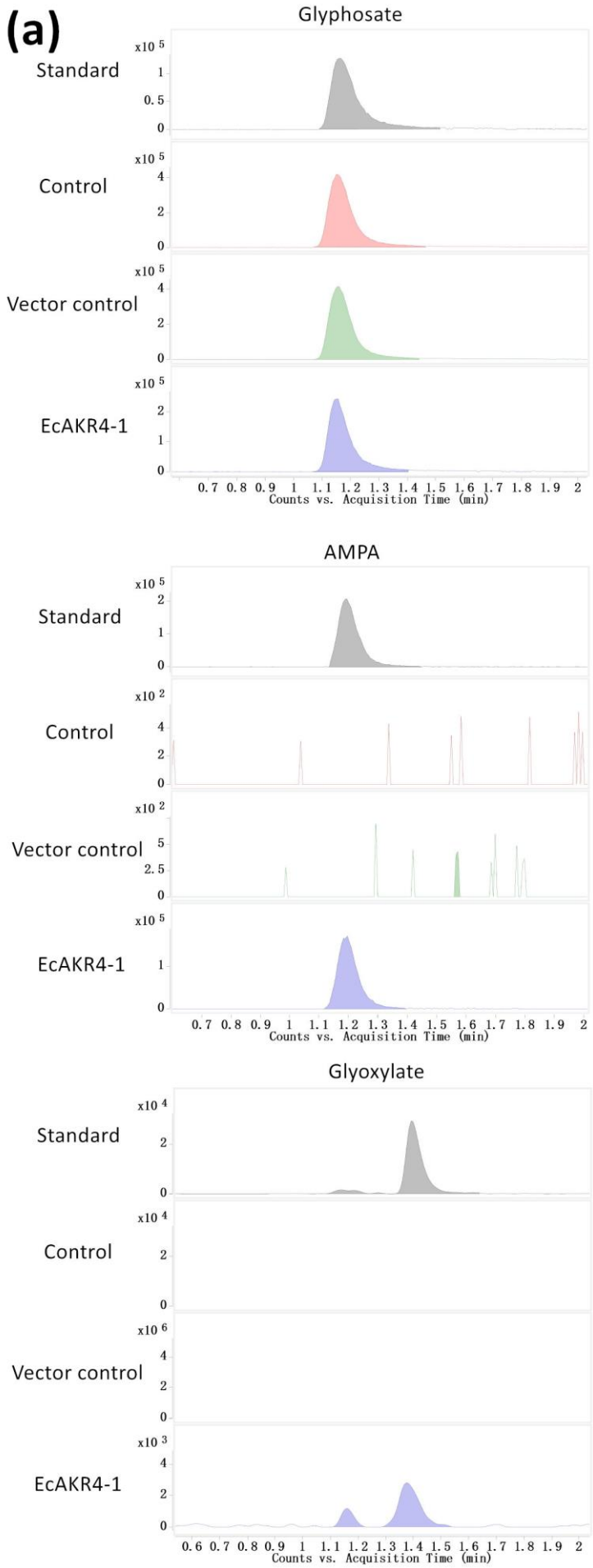

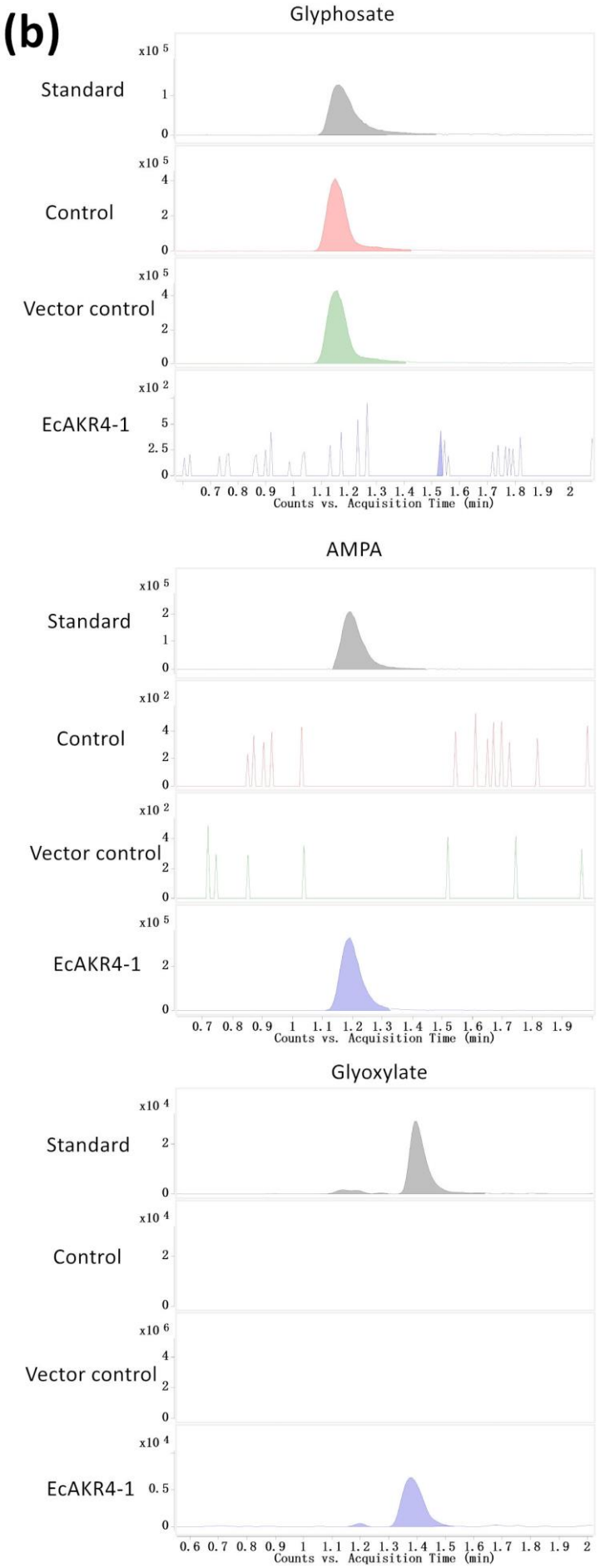

1

Fig. 3 HPLC-Q-TOF-MS analyses of glyphosate metabolism catalysed by *E. coli* expressed EcAKR4-1 at 1 h (a) and 5 h (b) after *in vitro* incubation. Standard: analytical grade glyphosate, aminomethylphosphonic acid (AMPA), and glyoxylate. Control: mixture of glyphosate and plant tissue extract. Vector control: mixture of *E. coli* expressed BSA protein, glyphosate and plant tissue extract. EcAKR4-1: mixture of *E. coil* expressed EcAKR4-1 enzyme, glyphosate and plant tissue extract.

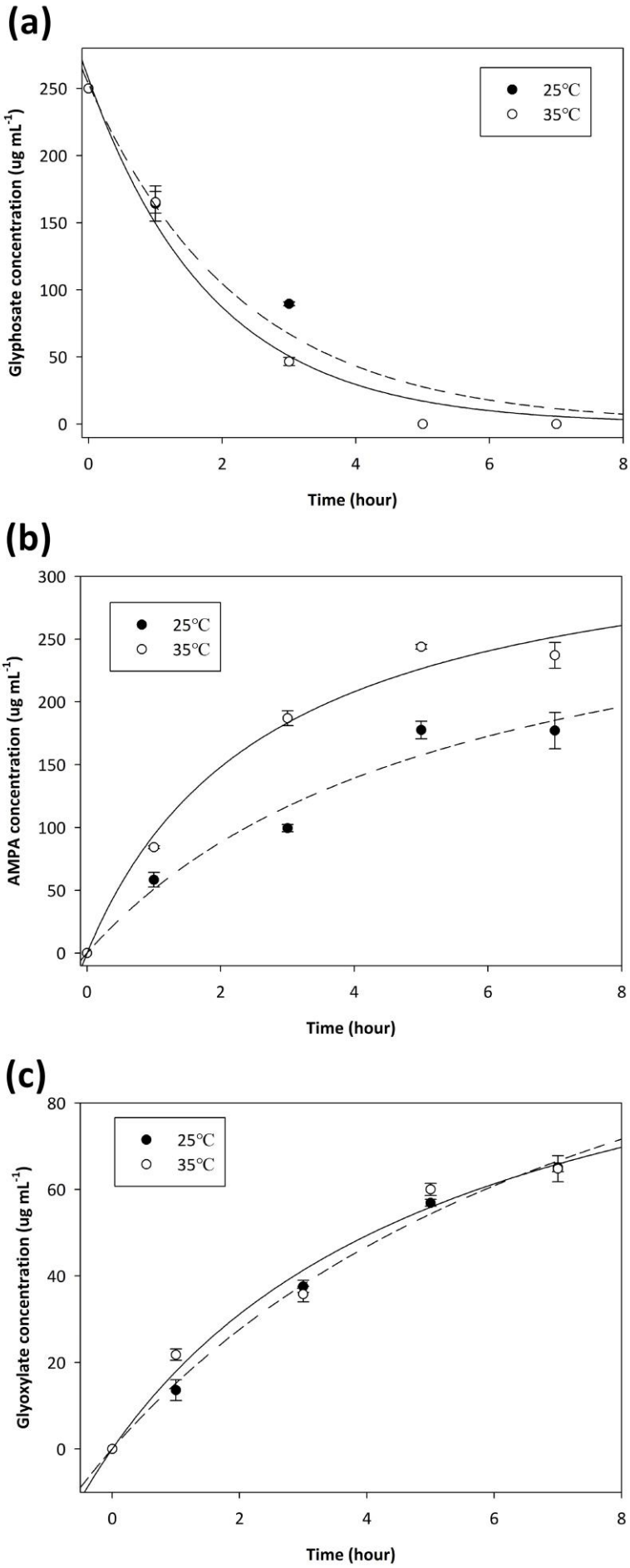

1

Fig. 4 Time-dependent glyphosate breakdown (a), and accumulation of glyphosate metabolites aminomethylphosphonic acid (AMPA) (b) and glyoxylate (c) in mixtures of *E. coli* expressed EcAKR4-1 and plant tissue extract. Data are means ±SE (n=6).

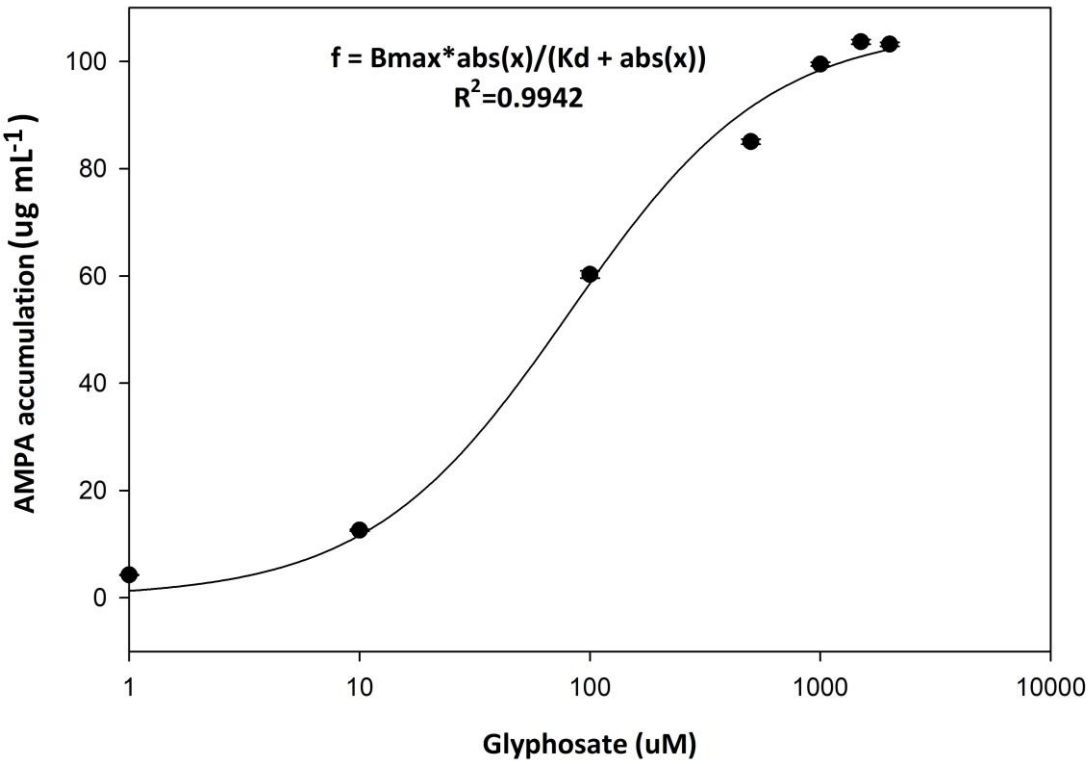

Fig. 5 Concentration-dependent accumulation of AMPA in response to increased glyphosate concentrations in the mixture of recombinant EcAKR4-1 enzyme and plant tissue extract. Data are means ±SE (*n*=6).

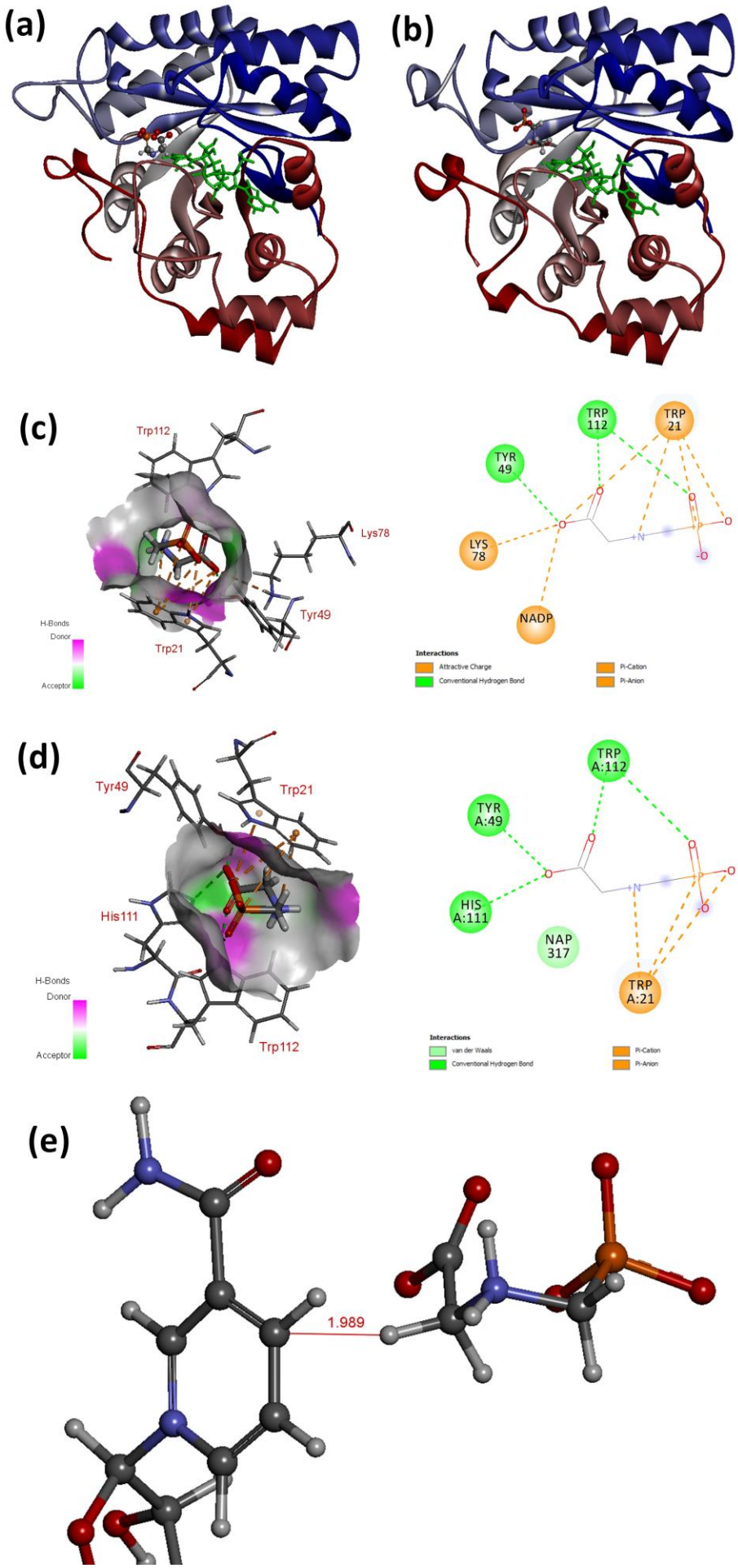

Fig. 6 3D modelling reveals structural interactions of EcAKR4-1 and glyphosate. General view of EcAKR4-1 with bound $NADP^+$ (stick representation colored in green) and glyphosate (ball and stick representation) in (a) Type 1 conformation, and (b) Type 2 conformation. (c) Spatial structure of contact interface between glyphosate and EcAKR4-1 in the type 1 conformation (left, NADP molecule is not present) and 2D-diagram (right) of intermolecular interactions. Protein contact surface is colored by H-bond donor/acceptor distribution, binding site amino acids represented by sticks, and intermolecular contacts indicated by dotted lines. (d) Spatial structure of contact interface between glyphosate and EcAKR4-1 in the type 2 conformation (left, NADP molecule is not present) and 2D-diagramm of intermolecular interactions (right). Protein contact surface is colored by H-bond donor/acceptor distribution, binding site amino acids represented by sticks, and intermolecular contacts indicated by dotted lines. (e) Partially presented relative spatial orientation of glyphosate (right) and $NADP^+$ (left). Distance between the transferable hydrogen and target carbon in the NADP composition is shown by a red line.

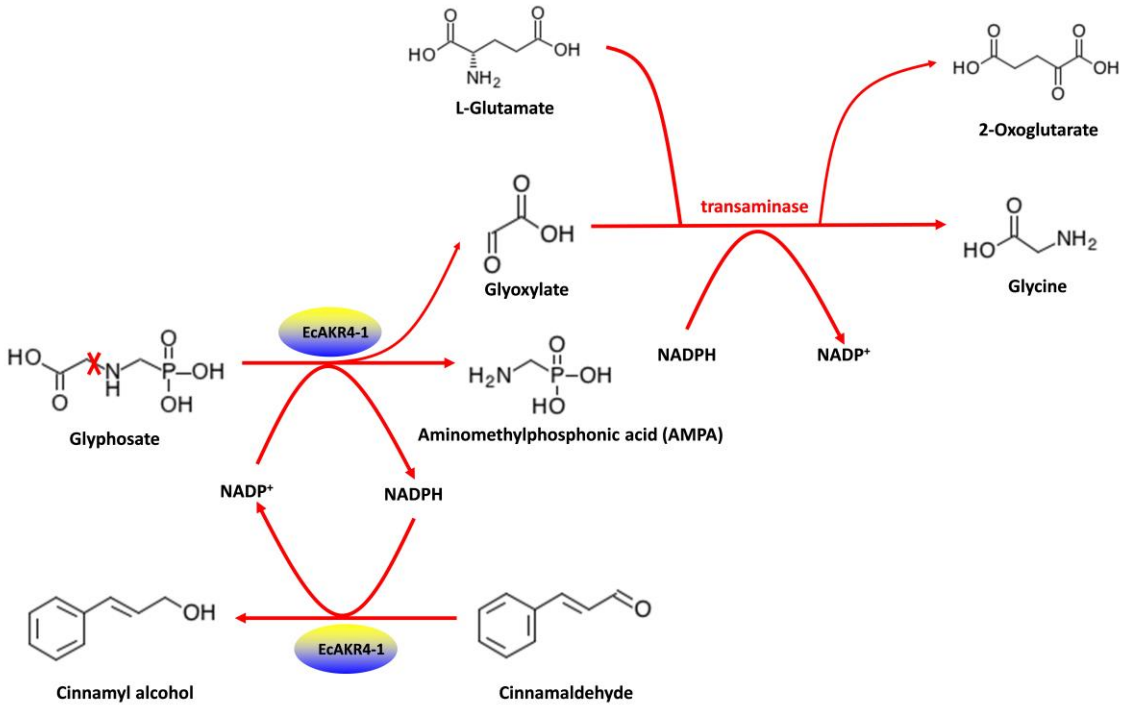

Fig. 7 Proposed metabolic pathway demonstrating the dual oxidase/reductase activity of EcAKR4-1 involved in glyphosate metabolism in *E. colona*. Glyphosate is oxidized to aminomethylphosphonic acid (AMPA) by EcAKR4-1 using $NADP^+$ as a cofactor, and meanwhile cinnamaldehyde is reduced to cinnamyl alcohol, regenerating $NADP^+$. Glyoxylate produced by glyphosate oxidation is further converted to glycine by transaminase coupled with L-glutamate reduction to 2-oxoglutarate with NADPH as a cofactor. X indicates cleavage of the C-N bond in the glyphosate molecule. Please note our structural modelling (Fig 6), in vitro glyphosate metabolism by *E. coli* expressed *EcAKR4-1* (Table 3), and metabolomics of *EcAKR4-1* transgenic rice (Table 6) are consistent with the proposed step for glyphosate conversion to AMPA. Further conversion of glyoxylate to glycine was only based on the metabolomic analysis of *EcAKR4-1* transgenic rice (Table 6). Nevertheless, further experimental validation is needed for the proposed pathway.

Parsed Citations

Agrawal C, Sen S, Yadav S, Rai S, Rai LC (2015) A novel aldo-keto reductase (AKR17A1) of Anabaena sp. PCC 7120 degrades the rice field herbicide butachlor and confers tolerance to abiotic stresses in E. coli. Plos One 10: e0137744
Pubmed: Author and Title
Google Scholar: Author Only Title Only Author and Title

Baerson SR, Rodriguez DJ, Minhtien T, Yongmei F, Biest NA, Dill GM (2002) Glyphosate-resistant goosegrass. Identification of a mutation in the target enzyme 5-enolpyruvylshikimate-3-phosphate synthase. Plant Physiol 129: 1265-1275
Pubmed: Author and Title
Google Scholar: Author Only Title Only Author and Title

Barrett KA, Mcbride MB (2005) Oxidative degradation of glyphosate and aminomethylphosphonate by manganese oxide. Environ Sci 39: 9223-9228
Pubmed: Author and Title
Google Scholar: Author Only Title Only Author and Title

Barry GF, Kishore GM (1995) Glyphosate tolerant plants. US patent 5, 463, 175
Pubmed: Author and Title
Google Scholar: Author Only Title Only Author and Title

Barski OA, Tipparaju SM, Bhatnagar A (2008) The aldo-keto reductase superfamily and its role in drug metabolism and detoxification. Drug Metab Rev 40: 553-624
Pubmed: Author and Title
Google Scholar: Author Only Title Only Author and Title

Bradford MMA (1976) A rapid and sensitive method for the quantitation on microgram quantities of protein utilizing the principle of protein-dye binding. Anal Biochem 72: 248–254
Pubmed: Author and Title
Google Scholar: Author Only Title Only Author and Title

Chu Z, Chen J, Nyporko A, Han H, Yu Q, Powles S (2018) Novel α-tubulin mutations conferring resistance to dinitroaniline herbicides in Lolium rigidum. Front Plant Sci 9
Pubmed: Author and Title
Google Scholar: Author Only Title Only Author and Title

de Carvalho LB, Alves PLdCA, González-Torralva F, Cruz-Hipolito HE, Rojano-Delgado AM, De Prado R, Gil-Humanes J, Barro F, Luque de Castro MD (2012) Pool of resistance mechanisms to glyphosate in Digitaria insularis. J Agric Food Chem 60: 615-622
Pubmed: Author and Title
Google Scholar: Author Only Title Only Author and Title

Délye C, Jasieniuk M, Le Corre V (2013) Deciphering the evolution of herbicide resistance in weeds. Trends Genet 29: 649-658
Pubmed: Author and Title
Google Scholar: Author Only Title Only Author and Title

Duhoux A, Carrère S, Gouzy Jm, Bonin L, Délye C (2015) RNA-Seq analysis of rye-grass transcriptomic response to an herbicide inhibiting acetolactate-synthase identifies transcripts linked to non-target-site-based resistance. Plant Mol Biol 87: 473-487
Pubmed: Author and Title
Google Scholar: Author Only Title Only Author and Title

Duke SO (2011) Glyphosate degradation in glyphosate-resistant and -susceptible crops and weeds. J Agric Food Chem 59: 5835-5841
Pubmed: Author and Title
Google Scholar: Author Only Title Only Author and Title

Duke SO, Powles SB (2008) Glyphosate: a once-in-a-century herbicide. Pest Manag Sci 64: 319-325
Pubmed: Author and Title
Google Scholar: Author Only Title Only Author and Title

Duke SO, Powles SB, Sammons RD (2018) Glyphosate-How it became a once in a hundred year herbicide and its future. Outlooks on Pest Manag 29: 247-251
Pubmed: Author and Title
Google Scholar: Author Only Title Only Author and Title

Gaines TA, Cripps A, Powles SB (2012) Evolved resistance to glyphosate in Junglerice (Echinochloa colona) from the tropical ord river region in Australia. Weed Technol 26: 480-484
Pubmed: Author and Title
Google Scholar: Author Only Title Only Author and Title

Gaines TA, Patterson EL, Neve P (2019) Molecular mechanisms of adaptive evolution revealed by global selection for glyphosate resistance. New Phytol doi:10.1111/nph.15858
Pubmed: Author and Title
Google Scholar: Author Only Title Only Author and Title

Gaines TA, Zhang W, Wang D, Bukun B, Chisholm ST, Shaner DL, Nissen SJ, Patzoldt WL, Tranel PJ, Culpepper AS, Grey TL, Webster

TM, Vencill WK, Sammons RD, Jiang J, Preston C, Leach JE, Westra P (2010) Gene amplification confers glyphosate resistance in Amaranthus palmeri. Proc Natl Acad Sci U S A 107: 1029-1034
Pubmed: Author and Title
Google Scholar: Author Only Title Only Author and Title

Ge X, d'Avignon DA, Ackerman JJH, Sammons RD (2010) Rapid vacuolar sequestration: the horseweed glyphosate resistance mechanism. Pest Manag Sci 66: 345-348
Pubmed: Author and Title
Google Scholar: Author Only Title Only Author and Title

Goh SS, Vila-Aiub MM, Busi R, Powles SB (2016) Glyphosate resistance in Echinochloa colona: phenotypic characterisation and quantification of selection intensity. Pest Manag Sci 72: 67-73
Pubmed: Author and Title
Google Scholar: Author Only Title Only Author and Title

Goh SS, Yu Q, Han H, Vila-Aiub MM, Busi R, Powles SB (2018) Non-target-site glyphosate resistance in Echinochloa colona from Western Australia. Crop Prot 112: 257-263
Pubmed: Author and Title
Google Scholar: Author Only Title Only Author and Title

González-Torralva F, Rojano-Delgado AM, Luque de Castro MD, Mülleder N, De Prado R (2012) Two non-target mechanisms are involved in glyphosate-resistant horseweed (Conyza canadensis L. Cronq.) biotypes. J Plant Physiol 169: 1673-1679
Pubmed: Author and Title
Google Scholar: Author Only Title Only Author and Title

Heap I (2019) International survey of herbicide resistant weeds [online]. In, Vol 2019, http: //www.weedscie nce.org
Pubmed: Author and Title
Google Scholar: Author Only Title Only Author and Title

Kavanagh KL, Mario K, Bernd N, Wilson DK (2002) The structure of apo and holo forms of xylose reductase, a dimeric aldo-keto reductase from Candida tenuis. Biochem 41: 8785
Pubmed: Author and Title
Google Scholar: Author Only Title Only Author and Title

Li J, Peng Q, Han H, Nyporko A, Kulynych T, Yu Q, Powles S (2018) A novel EPSPS Thr-102-Ser substitution endows glyphosate resistance in Tridax procumbens. Journal of Agricultural & Food Chemistry
Pubmed: Author and Title
Google Scholar: Author Only Title Only Author and Title

Lorrainecolwill, D. F, Powles, S. B, Hawkes, T. R, Hollinshead, P. H, Warner, S. AJ (2002) Investigations into the mechanism of glyphosate resistance in Lolium rigidum. Pestic Biochem Phys 74: 62-72
Pubmed: Author and Title
Google Scholar: Author Only Title Only Author and Title

Lu Y, Li Y, Yang Q, Zhang Z, Chen Y, Zhang S, Peng X-X (2014) Suppression of glycolate oxidase causes glyoxylate accumulation that inhibits photosynthesis through deactivating Rubisco in rice. Physiol Plantarum 150: 463-476
Pubmed: Author and Title
Google Scholar: Author Only Title Only Author and Title

Mattia P, Elena R, Gianluca M, Tommaso M, Carmelinda S, Beatrice V, Loredano P (2009) Glyphosate resistance by engineering the flavoenzyme glycine oxidase. J Biol Chem 284: 36415
Pubmed: Author and Title
Google Scholar: Author Only Title Only Author and Title

Nandula VK, Reddy KN, Rimando AM, Duke SO, Poston DH (2007) Glyphosate-resistant and -susceptible soybean (Glycine max) and canola (Brassica napus) dose response and metabolism relationships with glyphosate. J Agric Food Chem 55: 3540-3545
Pubmed: Author and Title
Google Scholar: Author Only Title Only Author and Title

Nandula VK, Riechers DE, Ferhatoglu Y, Barrett M, Duke SO, Dayan FE, Goldberg-Cavalleri A, Tétard-Jones C, Wortley DJ, Onkokesung N, Brazier-Hicks M, Edwards R, Gaines T, Iwakami S, Jugulam M, Ma R (2019) Herbicide metabolism: crop selectivity, bioactivation, weed resistance, and regulation. Weed Sci 67: 149-175
Pubmed: Author and Title
Google Scholar: Author Only Title Only Author and Title

Patterson EL, Pettinga DJ, Ravet K, Neve P, Gaines TA (2018) Glyphosate resistance and EPSPS gene duplication: Convergent evolution in multiple plant species. J Hered 109: 117-125
Pubmed: Author and Title
Google Scholar: Author Only Title Only Author and Title

Penning TM (2015) The aldo-keto reductases (AKRs): overview. Chem Biol Interact 234: 236-246
Pubmed: Author and Title
Google Scholar: Author Only Title Only Author and Title

Perotti VE, Larran AS, Palmieri VE, Martinatto AK, Alvarez CE, Tesio F, Permingeat HR (2019) A novel triple amino acid substitution in

the EPSPS found in a high-level glyphosate-resistant Amaranthus hybridus population from Argentina. Pest Manage Sci 75: 1242-1251
Pubmed: Author and Title
Google Scholar: Author Only Title Only Author and Title

Pizzul L, Castillo MDP, Stenström J (2009) Degradation of glyphosate and other pesticides by ligninolytic enzymes. Biodegradation 20: 751-759
Pubmed: Author and Title
Google Scholar: Author Only Title Only Author and Title

Pollegioni L, Schonbrunn E, Siehl D (2011) Molecular basis of glyphosate resistance-different approaches through protein engineering. Febs Journal 278: 2753-2766
Pubmed: Author and Title
Google Scholar: Author Only Title Only Author and Title

Powles SB, Lorrainecolwill DF, Dellow JJ, Preston C (1998) Evolved resistance to glyphosate in rigid ryegrass (Lolium rigidum) in Australia. Weed Sci 46: 604-607
Pubmed: Author and Title
Google Scholar: Author Only Title Only Author and Title

Powles SB, Yu Q (2010) Evolution in action: plants resistant to herbicides. Annu Rev Plant Biol 61: 317-347
Pubmed: Author and Title
Google Scholar: Author Only Title Only Author and Title

Pratley J, Stanton R, Urwin N, Baines P, Hudson D, Dill G, Bishop AC, Boersma M, Barnes CD (1999) Resistance to glyphosate in Lolium rigidum. I. Bioevaluation. Weed Sci 47: 405-411
Pubmed: Author and Title
Google Scholar: Author Only Title Only Author and Title

Reddy KN, Rimando AM, Duke SO, Nandula VK (2008) Aminomethylphosphonic acid accumulation in plant species treated with glyphosate. J Agric Food Chem 56: 2125
Pubmed: Author and Title
Google Scholar: Author Only Title Only Author and Title

Sammons RD, Gaines TA (2014) Glyphosate resistance: state of knowledge. Pest Manag Sci 70: 1367-1377
Pubmed: Author and Title
Google Scholar: Author Only Title Only Author and Title

Seiichi T, Naho H, Kazuko O, Haruko O, Akemi T, Seibi O, Hiroshi T (2010) Early infection of scutellum tissue with Agrobacterium allows high-speed transformation of rice. Plant J 47: 969-976
Pubmed: Author and Title
Google Scholar: Author Only Title Only Author and Title

Simpson PJ, Tantitadapitak CReed AM, Mather OC, Bunce CM, White SA, Ride JP (2009) Characterization of two novel aldo-keto reductases from Arabidopsis: expression patterns, broad substrate specificity, and an open active-site structure suggest a role in toxicant metabolism following stress. J Mol Biol 392: 465-480
Pubmed: Author and Title
Google Scholar: Author Only Title Only Author and Title

Sousa SMD, Rosselli LK, Kiyota E, Silva JCD, Souza GHMF, Peroni LA, Stach-Machado DR, Eberlin MN, Souza AP, Koch KE (2009) Structural and kinetic characterization of a maize aldose reductase. Plant Physiol Bioch 47: 98-104
Pubmed: Author and Title
Google Scholar: Author Only Title Only Author and Title

Vemanna RS, Vennapusa AR, Easwaran M, Chandrashekar BK, Rao H, Ghanti K, Sudhakar C, Mysore KS, Makarla U (2017) Aldo-keto reductase enzymes detoxify glyphosate and improve herbicide resistance in plants. Plant Biotechnol J 15: 794-804
Pubmed: Author and Title
Google Scholar: Author Only Title Only Author and Title

Venselaar H, Joosten RP, Vroling B, Baakman CAB, Hekkelman ML, Krieger E, Vriend G (2010) Homology modelling and spectroscopy, a never-ending love story. Eur Biophy J 39: 551-563
Pubmed: Author and Title
Google Scholar: Author Only Title Only Author and Title

Waterhouse A, Bertoni M, Bienert S, Studer G, Tauriello G, Gumienny R, Heer FT, De TB, Rempfer C, Bordoli L (2018) SWISS-MODEL: homology modelling of protein structures and complexes. Nucleic Acids Res 46: W296-W303
Pubmed: Author and Title
Google Scholar: Author Only Title Only Author and Title

Yu Q, Jalaludin A, Han H, Chen M, Sammons RD, Powles SB (2015) Evolution of a double amino acid substitution in the 5-Enolpyruvylshikimate-3-Phosphate synthase in Eleusine indica conferring high-level glyphosate resistance. Plant Physiol 167: 1440-1447
Pubmed: Author and Title
Google Scholar: Author Only Title Only Author and Title

Yu Q, Powles S (2014) Metabolism-based herbicide resistance and cross-resistance in crop weeds: A threat to herbicide sustainability

and global crop production. Plant Physiol 166: 1106-1118